Overexpression of ERCC6L correlates with poor prognosis and confers malignant phenotypes of lung adenocarcinoma

XIAOYUE HUANG[1*], LINGYU JIANG[2*], SUFANG LU[1*], MINGQING YUAN[1], HUI LIN[3], BAIJUN LI[3], ZHAOKE WEN[3] and YONGLONG ZHONG[3]

[1]Medical College, Guangxi University, Nanning, Guangxi Zhuang Autonomous Region 530004; [2]Intensive Care Unit and [3]Department of Thoracic Surgery, The People's Hospital of Guangxi Zhuang Autonomous Region, Guangxi Academy of Medical Sciences, Nanning, Guangxi Zhuang Autonomous Region 530021, P.R. China

Received January 7, 2022; Accepted May 9, 2022

DOI: 10.3892/or.2022.8342

Abstract. Excision repair cross-complementation group 6 like (ERCC6L) has been reported to be upregulated in a variety of malignant tumors and plays a critical oncogenic role. However, the role and molecular mechanism of ERCC6L in lung adenocarcinoma (LUAD) remain unclear, and were therefore investigated in the present study. Clinical data of patients with LUAD were obtained and bioinformatics analysis was performed to investigate the expression characteristics, prognostic value, and biological function of ERCC6L. In addition, cell function experiments were performed to detect the effect of ERCC6L silencing on the biological behavior of LUAD cells. The results revealed that ERCC6L expression was significantly higher in LUAD tissues vs. normal lung tissues and closely associated with nodal invasion, advanced clinical stage and survival in LUAD. Overexpression of ERCC6L was an independent prognostic biomarker of overall survival, progression-free interval, and disease-specific survival in patients with LUAD. DNA amplification and low methylation levels of ERCC6L suggested regulation at both the genetic and epigenetic levels. The most significant positive genes co-expressed with ERCC6L were mainly enriched in the cell cycle signaling pathway. The major functions of ERCC6L in LUAD cells were positively correlated with the cell cycle, DNA damage, DNA repair, proliferation, invasion and epithelial-mesenchymal transition (EMT). Knockdown of ERCC6L inhibited the proliferative, migratory and invasive abilities of A549 and PC9 cells. It also promoted cell apoptosis, and led to cell cycle arrest in the S phase. ERCC6L may regulate the EMT process through the Wnt/β-catenin and Wnt/Notch 3 signaling pathways, thus regulating the tumorigenesis and progression of LUAD. The overexpression of ERCC6L may be a biological indicator for the diagnosis and prognosis of LUAD. ERCC6L may be a novel molecular target for the treatment of lung cancer.

Correspondence to: Dr Yonglong Zhong or Dr Zhaoke Wen, Department of Thoracic Surgery, The People's Hospital of Guangxi Zhuang Autonomous Region, Guangxi Academy of Medical Sciences, 6 Taoyuan Road, Nanning, Guangxi Zhuang Autonomous Region 530021, P.R. China
E-mail: yl.zhong@foxmail.com
E-mail: jilihcwl@sina.com

*Contributed equally

Key words: excision repair cross-complementation group 6 like, lung adenocarcinoma, bioinformatics analysis, prognosis, epithelial-mesenchymal transition

Introduction

Lung cancer has the highest rates of morbidity and mortality among cancers worldwide (1). Lung adenocarcinoma (LUAD) is the most common pathologic type and a highly invasive and lethal type of cancer. Early-stage LUAD can easily invade blood vessels and lymphatic vessels. Clinically, patients with early-stage cancer do not have obvious symptoms, often, the tumor has metastasized prior to causing the corresponding symptoms. Therefore, most patients with LUAD miss the optimal time for treatment. In recent years, great improvements have been achieved in the diagnosis and treatment of LUAD. However, the long-term survival rate of patients with LUAD remains low (2), and the local progression, recurrence, and metastasis of tumors are the main reasons for poor prognosis. Therefore, it is of great significance to further investigate biomarkers related to the diagnosis and prognosis of LUAD in order to improve the overall efficacy of treatment against lung cancer (3).

Excision repair cross-complementation group 6 like (ERCC6L) is a newly discovered DNA helicase (4), also termed polo kinase 1 interaction checkpoint helicase (PICH). It has been demonstrated that ERCC6L is a member of the ERCC6 subfamily, SNF2 (5). Previous research has revealed that the ERCC6L protein is related to embryonic development, indicating that ERCC6L may play an important role in maintaining growth (6). In addition, Baumann *et al* revealed that ERCC6L binds to a mitogen-regulated kinase [polo-like kinase 1 (PLK1)] and is involved in remodeling centromeric chromatin (7). PLK1 regulates cell division and proliferation, and is considered a genetic marker for tumor development (8,9). Dysfunction of ERCC6L induces DNA damage that affects the

cell division and cycle, potentially promoting the development of cancer (10,11). In recent years, continuous research has shown that ERCC6L appears to play a critical role in tumorigenesis and progression (12). For example, ERCC6L is overexpressed in breast and kidney cancers and is significantly associated with poor prognosis. ERCC6L was found to be upregulated in hepatocellular carcinoma, neuroblastoma, gastric cancer and colorectal cancer, and silencing of ERCC6L inhibited cancer cell growth, invasion, metastasis and the EMT process. Furthermore, aberrant expression of ERCC6L promotes tumor progression via the PI3K/AKT and NF-κB pathways. This evidence has demonstrated that ERCC6L may be a valuable biomarker of tumors and may act as an important mediator in the malignant biological behavior of tumors. However, the role of ERCC6L in the development of LUAD and its underlying molecular mechanism remain unknown. In the present study, the expressions profiles and clinical significance of ERCC6L in LUAD were investigated. In addition, the biological functions and molecular mechanism of ERCC6L, involved in the tumor progression of LUAD were explored *in vitro* and *in vivo*.

Materials and methods

Materials. Paraffin tissue specimens were obtained from the People's Hospital of Guangxi Zhuang Autonomous Region (Nanning, China) from October 2010 to September 2012. The clinicopathological data of 85 patients with LUAD were obtained from the Department of Pathology of the hospital. The extracted information included age, sex, tumor size, lymph node metastasis, TNM stage, pathological grade and life status. The histological staging was based on the 2018 edition of the World Health Organization (WHO), and the tumor staging was based on the 8th edition of the American Joint Committee on Cancer (AJCC) (13). Patients with LUAD included in the present study did not receive any antitumor treatment preoperatively, develop infectious diseases, or expire within one month after surgery. Follow-up data, including outpatient follow-up and telephone follow-up, were collected from the electronic follow-up system established by the department; data collection was initiated one month after surgical treatment of the patient and ended in mid-2019. Cancer tissue was defined as the solid non-necrotizing tissue of the tumor; normal lung tissue adjacent to the cancer was defined as the lung tissue 5 cm away from the edge of the tumor. The tissue samples were fixed with 10% neutral formalin for 24 h at room temperature (RT), embedded in paraffin, and then serially sectioned at 5 μm. All sections were preserved by the scientific research laboratory following standard procedures. The present study was approved (approval no. KY-KJT-2021-125) by the Ethics Committee/Institutional Review Committee of the People's Hospital of Guangxi Zhuang Autonomous Region and all participants provided written informed consent in accordance with the Declaration of Helsinki. The histopathological results were reviewed by two experienced pathologists.

Methods

Immunohistochemical assay. Grilled paraffin slices at 60˚C for 2 h; For dewaxing and hydration, the sections were placed in xylene lotion and soaked for 20 min in 100, 95, 90, 85, and 80% ethanol. For antigen repair, 1X citric acid repair solution (pH 6.0) was boiled in a pressure cooker for 3 min, and cooled with water for 10 min. To eliminate endogenous peroxidase activity, 3% H_2O_2 (50 μl) was added, and the sections were incubated at RT for 10 min. The sections were blocked in goat serum (1:10; product code SL038; Beijing Solarbio Science & Technology Co., Ltd.) and incubated at RT for 15-20 min. Following washing with phosphate-buffered saline (PBS), the sections were incubated with 50 μl of rabbit anti-human ERCC6L polyclonal antibody (1:200; cat. no. PA5-62199; Invitrogen; Thermo Fisher Scientidic, Inc.) at 4˚C overnight. To display antigen distribution, the sections were incubated with 50 μl of ready-use Max Vision™ HRP-polymer anti-rabbit reagent (cat. no. KIT-5001; Fuzhou Maixin Biotech Co., Ltd.) for 15 min at RT, closed with a warm box, and rinsed with PBS. Subsequently, freshly prepared 3,3'-diaminobenzidine solution was added for color development. The sections were then incubated in hematoxylin dye for 2 min at RT, and excess dye was removed by rinsing. Subsequently, the sections were differentiated in hydrochloric acid for 5 sec, submerged in ammonia solution for 5 min, and rinsed with water. The slices were dehydrated in gradient alcohol (80, 85, 90,95, and 100%) for 10 min and soaked in xylene lotion for 10 min. After sealing with neutral gum, the sections were observed and photographed under a light microscope(magnification, x200; Olympus MX51; Olympus Corporation).

Clinical sample analysis. To identify potential biomarkers of LUAD, the association between the expression of ERCC6L, malignant pathological features, and overall survival (OS) in 85 clinical LUAD samples were analyzed. The clinical samples were divided into two groups, namely high- and low-ERCC6L expression groups, according to the median expression of ERCC6L mRNA.

Data mining. Normal samples from the tumor database of The Cancer Genome Atlas (TCGA; https://cancergenome.nih.gov/) were integrated to identify the expression characteristics of ERCC6L mRNA. From TCGA database, 514 cases of primary LUAD and 59 cases of normal controls were collected. ERCC6L mRNA expression and clinicopathological characteristics were analyzed. Of the 514 patients, 505 had complete clinical and follow-up information. The role of ERCC6L mRNA expression in patients with LUAD was determined through analysis of TCGA clinical data of those 505 patients. The extracted data included age, sex, smoking history, tumor size, lymph node infiltration, distant metastasis, TNM stage, residual tumor, recurrence status, life status, OS, progression-free interval (PFI), disease-free interval (DFI) and disease-specific survival (DSS).

Two lung cancer gene microarray datasets (GSE31210 and GSE30219) (14,15) were downloaded from the Gene Expression Omnibus (GEO; https://www.ncbi.nlm.nih.gov/geo/), to validate the expression and clinical significance of ERCC6L.

Genetic and epigenetic analysis. To investigate the mechanism of ERCC6L dysregulation in LUAD, its gene-level threshold Gistic2.0-processed copy number variation (CNV) (16) (n=511) and DNA methylation status (n=453, methylation 450K) were concurrently collected from TCGA. Data on ERCC6L mRNA expression, copy number, and DNA methylation in LUAD cell

lines were obtained from the Cancer Cell Line Encyclopedia (CCLE) (https://dashela.broad institute.org/ccle) (17,18). This is an online database that provides public access, analysis, and visualization of genomic data (e.g., gene expression, gene methylation, and mutation data) for >1,100 cell lines. UALCAN Network (http://ualcan.path.uab.edu) (19) was used to analyze the level of ECRR6L promoter methylation in tumor tissue and normal tissue.

Identification of differentially expressed genes associated with ERCC6L in LUAD. LinkedOmics (http://www.linkedomics.org) (20) is a new open portal offering multiple omics data analysis of all 32 types of cancer included in TCGA. In the present study, it was used to identify differentially expressed genes related to ERCC6L in LUAD. A Benjamini-Hochberg false discovery rate (FDR) <0.01 and P-value <0.05 were set as critical criteria. The top three factors that were positively correlated with ERCC6L were selected for further analysis. Pearson's correlation was conducted to analyze the expression between ERCC6L and selected genes. Gene Expression Profiling Interactive Analysis 2 (GEPIA2; http://gepia2.cancer-pku.cn) (21) is an online interactive web server that obtains RNA sequencing data from tumor and normal samples in TCGA and the Genotype-Tissue Expression Project for analysis of the expression profile and prognostic value of selected genes. Patients with LUAD were grouped according to the median mRNA expression. P-values <0.05 denoted statistically significant differences.

Functional and pathway enrichment analysis. Gene set enrichment analysis (GSEA) using the LinkInterpreter module of LinkedOmics (22) was performed for ERCC6L and its co-expressed genes using TCGA RNA-sequencing (RNA-seq) data. Analysis of Kyoto Encyclopedia of Genes and Genomes (KEGG) (23) and Gene Ontology (GO) (24) pathways (e.g., cellular components, molecular functions, and biological processes) identified potential pathways of ERCC6L. FDR <0.05 and P-value <0.05 denoted statistically significant differences.

Single-cell level analysis. The cancer single-cell state atlas (CancerSEA; http://biocc.hrbmu.edu.cn/CancerSEA/) (25) was used to investigate the function of cancer cells of different states at the single-cell level. This analysis was conducted to reveal significant differences in enrichment using data from the Molecular Signatures Database (MSigDB) (https://www.gsea-msigdb.org/gsea/msigdb) and analyze the function of ERCC6L. For each single-cell dataset derived from circulating tumor cells, the Spearman rank correlation test was used to analyze the significant correlation between gene expression and functional status; multiple comparisons were corrected for FDRs.

Cell culture. Human LUAD cell lines (A549, PC9, and H1975) and 293T cells were obtained from the Typical Culture Preservation Committee of the Chinese Academy of Sciences (Shanghai, China). The culture conditions of the three cell lines were: 10% Fetal bovine serum, 1% streptomycin, and RPMI-1640 medium. The cells were cultured at 37˚C in 5% CO_2. The reagents were purchased from Thermo Fisher Scientific, Inc. (GIBCO-BRL; Invitrogen; Thermo Fisher Scientific, Inc.).

Lentivirus design and cell transfection. Suzhou GenePharma Co., Ltd. was commissioned to design and construct a lentiviral vector for the target gene. The lentivirus RNAi vector was LV-3 of a four-plasmid system. The LV3 (H1/GFP-Puro) vector was synthesized for the lentivirus-short hairpin-ERCC6L (Lv-shRNA-ERCC6L). RNA interference target (sh-ERCC6L) was designed according to the sequence of the ERCC6L gene and a GV248-GFP-lentiviral vector was used as a negative control (sh-NC). The sh-ERCC6L sequence was 5'-GGTGGTGTCGGTTTAACATTA-3', while that of the sh-NC sequence was 5'-TTCTCCGAACGTGTCACGGT-3'. A total of three lentivirus packaging plasmids were used to transfect into 293T cells. The released virus was harvested and concentrated by ultracentrifugation at 40,000 g for 2 h at 4˚C. The titer of the lentivirus was $5x10^8$ TU/ml. A549 and PC9 cells were transfected with the lentivirus at a multiplicity of infection (MOI) of 10 with 5 μg/ml polybrene (product no. H9268; Sigma-Aldrich; Merck KGaA). The enhanced GFP gene was integrated into the transfected plasmid to distinguish the successful transfection of cells. The stable expressing cells were screened by treating with 4 μg/ml puromycin (product no. P8833; Sigma-Aldrich; Merck KGaA) for 2 weeks.

RNA extraction and reverse transcription-quantitative polymerase chain reaction (RT-qPCR). Collected transfected A549 and PC9 cells were added with an appropriate amount of TRIzol reagent (Beijing Solarbio Science & Technology Co., Ltd.). Total RNA extraction was performed according to the instructions provided by the manufacturer. After the RNA was diluted with RNase-free water, 1 μl was added to the NanoDrop-2000 micro-nucleic acid detector to determine the absorbance, and the samples were stored at -80˚C. cDNA was synthesized according to the manufacturer's instructions using a reverse transcription kit [PrimeScript™ RT reagent Kit with gDNA Eraser (Perfect Real Time), cat. no. RR047A; Takara Bio, Inc.]. Real-time PCR was then performed using SYBR-Green qPCR Master Mix (Takara Bio, Inc.) on an ABI 7500 real-time quantitative fluorescence PCR system (Applied BioSystems; Thermo Fisher Scientific, Inc.). Briefly, the qPCR cycling condition were an initial denaturation step at 95˚C for 30 sec, followed by an annealing with 40 cycles at a melting temperature of 95˚C for 5 sec, and an extension with 40 cycles at a temperature of 60˚C for 34 sec. The RT-qPCR primers for ERCC6L and GAPDH were purchased from Sangon Biotech Co., Ltd. The specific primers used were as follows: ERCC6L forward, 5'-tcctcctcacaggaacccca-3' and reverse, 5'-ccag-cagggacccttgacaa-3'; GAPDH forward, 5'-CATGAGAAGTAT GACAACAGCCT-3' and reverse, 5'-AGTCCTTCCACGATA CCAAG-3'. GAPDH was used as the internal control, and the results were analyzed using the $2^{-\Delta\Delta Cq}$ method (26).

Western blot analysis. Radioimmunoprecipitation (RIPA) assay protein extraction reagent and 10 g/l benzene methyl sulfonyl fluoride (both from Beyotime Institute of Biotechnology) were used to lyse H1975, PC9, and A549 cells. A BCA protein detection kit was used to determine the protein concentration (Beyotime Institute of Biotechnology). Appropriate samples and

molecular weight standard marker were absorbed and slowly added into the glue hole. An equal volume of 1X loading buffer was added to the swimming lanes on both sides of the sample. Electrophoresis was performed at 80 V for approximately 20 min and at 120 V for approximately 90 min. The proteins (10 μg) were separated using 10% SDS-PAGE and transferred to polyvinylidene difluoride membranes. The membranes were blocked with 5% skim milk (high-protein skim high-calcium milk powder; Yili Co., Ltd., Inner Mongolia, China) for 2 h at RT. Subsequently, the membrane was incubated with Tris-buffered saline containing 0.5% Tween-20 (TBST) (Beyotime Institute of Biotechnology) solution containing anti-ERCC6L antibody (1:1,000; cat. no. 15688-1-AP), neural-cadherin (N-cadherin; 1:2,000; cat. no. 22018-1-AP), epithelial cadherin (E-cadherin; 1:5,000; cat. no. 20874-1-AP), vimentin (1:2,000; cat. no. 10366-1-AP), snail family transcriptional repressor 1 (Snai1; 1:500; cat. no. 13099-1-AP), snail family transcriptional repressor 1 (Snai2; 1:500; cat. no. 12129-1-AP), notch receptor 3 (Notch 3; 1:500; cat. no. 55114-1-AP), β-catenin (1:5,000; cat. no. 51067-2-AP), GAPDH (1:5,000; cat. no. 10494-1-AP) at 4˚C for 12 h. All antibodies were purchased from Wuhan Sanying Biotechnology. Subsequently, after washing with TBST, the membrane was incubated with horseradish peroxidase-labeled anti-rabbit antibodies (1:5,000; bs-80295G-HRP; BIOSS) at RT for 2 h. The proteins were visualized using the Odyssey FC imaging system (LI-COR Biosciences).

Cell proliferation assay. Transfected A549 and PC9 cells were cultured in 96-well plates (1,500 cells/well) and transfected for 0, 24, 48, 72 and 96 h, respectively. A total of 20 μl Cell Counting Kit-8 (CCK-8) reagent (Dojindo Laboratories, Inc., Japan) was added to part of the cells in darkness. Following incubation for 2 h, the optical density value for each well at 450 nm was detected using a microplate instrument (Thermo Fisher Scientific, Inc.).

Colony formation assay. Suspended transfected A549 and PC9 cells were seeded into a six-well plate at a density of 500 cells/ml. The culture was terminated when white clones in the plate were visually observed. The cells were cultured at 37˚C and 5% CO_2 for 14 days. Next, 1 ml of 0.5% crystal violet solution (Beijing Solarbio Science & Technology Co., Ltd.) was added to each well after cells were fixed by pure methanol at RT, and then the cells were stained for 30 min at RT. Subsequently, the number of clones was recorded. The number of cells per clone consisted of >50 cells.

Apoptosis and cell cycle assay. In this study, the Annexin V-fluorescein isothiocyanate/propidium iodide (Annexin V-FITC/PI; Nanjing KeyGen Biotech Co., Ltd.) method was used to detect cell apoptosis by flow cytometry. Transfected A549 and PC9 cells were collected, and 3-5x10^5/ml resuspended cells were placed in a centrifuge tube. Following centrifugation at 300 x g for 5 min at RT, binding buffer (500 μl) was added to resuspend the cells. After adding 5 μl of Annexin V-allophycocyanin, the cells were incubated for 5-10 min. Next, PI dye solution (5 μl) was added and mixed. The solution was incubated at RT for 5-15 min in the dark. Flow cytometry (BD FACSCanto™ II) was performed, and the data were analyzed using FlowJo VX software (FlowJo LLC).

Similarly, transfected A549 and PC9 cells were collected and fixed with anhydrous ethanol until the final concentration was 75% at 4˚C overnight. The cells were then incubated overnight at 4˚C. The following day, PI/RNase Staining Buffer (0.5 ml; BD Biosciences) was added. Following incubation at RT for 15 min in the dark, the cells were fully mixed and examined using flow cytometry (BD FACSCanto™ II). The results of the cell cycle were analyzed using the Modfit LT 3.1 software (Verity Software House, Inc.).

Wound healing assay. Approximately 8x10^5 transfected A549 and PC9 cells were added into each well of a six-well plate, allowed to reach a density >90%, and then cultured in serum-free medium. Horizontal lines were marked evenly at the back of the six-well plate (every 0.5-1 cm), crossing the wells. At least five lines crossed each well. Images were captured at 0, 24 and 48 h using a fluorescence microscope (magnification, x200; Olympus IX71; Olympus Corporation). The ImageJ software (version 1.8.0; National Institutes of Health) was used to analyze the wound healing. The experiment was performed thrice.

Cell migration assay. Transfected A549 and PC9 cells were collected and their density was adjusted to 2-3x10^5/ml. The cell migration assay was carried out using an 8.0-μm pore size Transwell chamber (product number 3422; Corning, Inc.). In the lower chamber, complete medium containing 15% fetal bovine serum (600 μl) was added. In the upper chamber, cell suspension (100 μl) was added. Following incubation with 5% CO_2 at 37˚C for 18-24 h, the compartment was removed using tweezers. The fluid in the upper compartment was drained, and the cells on the surface of the basement membrane of the upper compartment were gently removed using a wet cotton swab. The chamber was moved to the well containing 600 μl of methanol; the cells were fixed at RT for 30 min and stained with 600 μl of 0.1% crystal violet dye for 20 min at RT. The bottom membrane of the chamber was gently cut with a razor blade and allowed to dry. Following transfer to a slide, one drop of neutral resin was added, and the slide was covered with a cover glass. Five visual fields were randomly selected for counting under a fluorescence microscope (magnification, x200; Olympus IX71).

Cell invasion assay. A 24-well plate with a small chamber containing an 8.0-μm pore size Matrigel-coated membrane (product number 354480; BioCoat™ Matrigel®; BD Biosciences) was used for the A549 and PC9 cells invasion assay. The BioCoat Matrigel invasion chambers were rehydrated with warm (37˚C) serum-free medium for 30 min at RT according to the manufacturer's instructions. Following rehydration, the medium was carefully removed. Cells were collected and their density was adjusted to 2-3x10^5 cells/ml. Serum-free medium (200 μl) was added to the upper chamber of the 24-well plates for activation for 30 min; complete medium with 15% serum (600 μl) was added to the lower chamber. Subsequently, cell suspension (100 μl) was added to the upper chamber, and the cells were incubated with 5% CO_2 for 30-34 h at RT. The upper compartment fluid was blotted, and the cells on the surface of the upper compartment substratum were gently removed using a wet cotton swab. The subsequent operations were analogous to the cell migration assay.

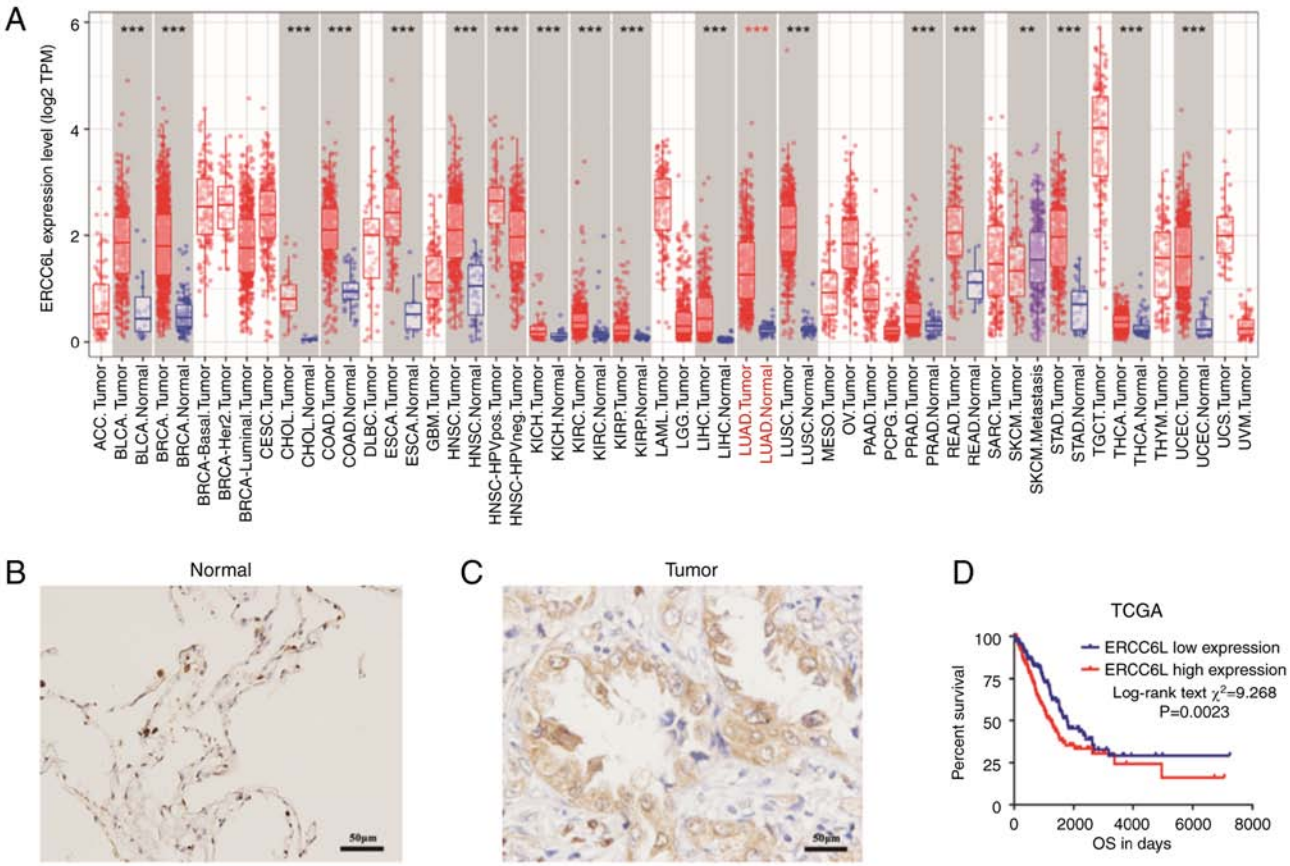

Figure 1. Expression profile of ERCC6L in pan-cancer and LUAD. (A) The expression of ERCC6L gene in pan-cancers based on the TCGA database. (B and C) ERCC6L protein expression was detected by immunohistochemical detection. Representative images of ERCC6L protein staining in (B) normal lung tissue and (C) LUAD tissue. (D) Survival analysis of ERCC6L protein expression and overall survival in 85 patients with LUAD. **P<0.01 and ***P<0.01. ERCC6L, excision repair cross-complementation group 6 like; LUAD, lung adenocarcinoma; TCGA, The Cancer Genome Atlas; OS, overall survival.

Establishment of a mouse xenograft model of LUAD. A mouse xenograft model of LUAD was performed under the guidance of the Ethics Committee, combining methods previously described (27-29). The animal experiment of this study was approved (approval no. 202103009) by The Animal Care and Welfare Committee of Guangxi Medical University (Nanning, China). The BALB/c nude mice were raised at the Experimental Animal Center of Guangxi Medical University under specific-pathogen free (SPF) conditions, with a constant temperature (20-24˚C) and humidity (45-65%) and a 12-h light-dark cycle. All nude mice were provided with food and sterile water *ad libitum*. A total of 14 female mice (four weeks old; weight, 10-12 g) were divided into a sh-ERCC6L group and a sh-NC group (n=7 mice per group). A total of $2x10^6$ cells transfected with either sh-ERCC6L or sh-NC were subcutaneously injected into the right armpit of each mouse. The mice were monitored daily and tumor volumes were recorded every 4 days. After 15 days of inoculation, the nude mice were anesthetized by intraperitoneal injection of 4% chloral hydrate (200 mg/kg) and intramuscular injection of ketorolac (1mg/kg; painkiller), and then euthanized by cervical dislocation. The final volume and weight of the tumors were measured. The tumor volume was calculated as: (Length x width^2)/2.

Data processing and statistical analysis. The SPSS Statistics 20.0 software (IBM Corp.) was used for statistical analysis. Quantitative data were presented as the mean ± standard deviation. Welch's t-test (for unpaired samples) and χ^2 test were performed to determine the association between the mRNA levels of ERCC6L and clinicopathological features. For patients with duplicated ERCC6L expression data, the median values were selected for analysis. The receiver operating characteristic (ROC) curve was used to determine the diagnostic and prognostic value of ERCC6L expression in LUAD. Kaplan-Meier curves for OS, PFI, DFI, and DSS were generated using the GraphPad Prism 8.0.2 (GraphPad Software, Inc.) software. The significant difference between the survival curves was identified by log-rank testing. Univariate and multivariate Cox regression analyses were performed to determine the independent prognostic factors. P-values <0.05 were considered to indicate statistically significant differences.

Results

Expression profiles of ERCC6L in pan-cancer and LUAD tissues. The pan-cancer RNA-seq data of ERCC6L was first extracted from TCGA database, and the mRNA expression levels of ERCC6L were analyzed in primary tumors and normal solid tissues with a sample size of ≥3. The results revealed that ERCC6L mRNA was upregulated in most human malignant solid tumors including LUAD, and it may be involved in the occurrence and development of cancers (Fig. 1A). The

Table I. Association of the clinicopathological parameters between high and low ERCC6L expression groups in 85 patients with LUAD.

	ERCC6L expression			
Parameters	Low (n=46)	High (n=39)	χ^2/t	P-value
Age (years)			<0.001	0.995
≤65	33	28		
>65	13	11		
Sex			1.708	0.191
Male	23	25		
Female	23	14		
Tumor size			0.805	0.369
T1-2	12	7		
T3-4	34	32		
Nodal invasion			5.662	0.017[a]
No	26	12		
Yes	20	27		
Clinical stage			5.108	0.024[a]
I/II	29	15		
III/IV	17	24		
Pathology grade			2.419	0.120
I/II	33	23		
III	11	16		
Living status			6.830	0.009[a]
Alive	19	6		
Dead	27	33		

[a]P<0.05. ERCC6L, excision repair cross-complementation group 6 like; LUAD, lung adenocarcinoma.

expression of ERCC6L protein in paraffin tissue samples of LUAD from our hospital was then detected by immunohistochemistry. The results showed that the alveolar epithelial cells of normal lung tissue exhibited negative or weak positive staining (Fig. 1B), while the tumor tissue exhibited strong positive expression (brown color) (Fig. 1C). Collectively it was demonstrated that the expression of ERCC6L protein was significantly higher in LUAD tissues.

Association between ERCC6L protein expression and clinicopathological features in patients with LUAD. The expression of ERCC6L in patients with LUAD divided into the high- and low-expression groups according to the median, and the association between the expression of ERCC6L and the clinical characteristics of patients was analyzed (Table I). The results showed that ERCC6L protein expression was significantly higher in tumor tissues of patients with positive nodal invasion (N1/2/3; P=0.017) or advanced TNM stage (III/IV; P=0.024), and those who expired (P=0.009). However, high ERCC6L expression was not associated with age, sex, tumor size, or pathological grade. To investigate whether ERCC6L expression was associated with patient prognosis, clinical follow-up information was extracted, and OS was used as the endpoint. Kaplan-Meier analysis revealed that patients with high ERCC6L expression in lung glands had poor OS (P=0.0023; Fig. 1D). Subsequently, Cox regression analysis was conducted to evaluate the prognostic value of ERCC6L in patients with LUAD (Table II). Univariate regression analysis showed that OS was significantly associated with high ERCC6L expression (P=0.002), nodal invasion (P<0.001), and tumor size (P=0.025) in LUAD. Multivariate regression analysis further confirmed that high ERCC6L expression (P=0.035) and nodal invasion (P=0.005) were independent prognostic factors of poor OS in patients with LUAD.

Association between ERCC6L mRNA expression and clinicopathological features in patients with LUAD based on TCGA database. RNA-seq data of LUAD was extracted from the TCGA database for further analysis with a larger sample size. The association between the mRNA expression levels of ERCC6L and clinicopathological parameters in 514 LUAD tissues and 59 normal lung tissues was analyzed. The results suggested that ERCC6L mRNA expression was significantly upregulated in LUAD tissues (Fig. 2A). Owing to individual differences between patients, the mRNA expression of ERCC6L in cancer tissues and normal tissues of the same patient was compared (Fig. 2B). This comparison confirmed the overexpression of ERCC6L mRNA in LUAD tissues. As revealed in Fig. 2C-I, the data analysis revealed that the mRNA expression of ERCC6L was significantly upregulated in patients with smoking history, positive nodal invasion and advanced clinical staging, as well as those who expired, irrespective of sex, tumor size and distal metastasis. In addition, although the expression levels of ERCC6L mRNA appeared to be higher in residual and recurrent tumors, no significant differences were observed. (Figs. 2J and S1).

Association between ERCC6L mRNA expression and outcome of patients with LUAD. To investigate the prognostic value of ERCC6L mRNA expression in LUAD, the OS, PFI, DFI, and DSS was analyzed in the TCGA cohort. Kaplan-Meier analysis demonstrated that patients with LUAD with high ERCC6L mRNA expression in the TCGA-LUAD cohort had poor OS, DFI, DSS, and PFI (Fig. 2K-N). Subsequently, Cox regression analysis was performed to further determine whether ERCC6L was an independent risk factor in patients with LUAD. As revealed in Table III, in terms of OS, univariate analysis showed that clinical stage, residual tumor, and ERCC6L mRNA expression were associated with OS (P<0.001, P<0.001, and P=0.003, respectively). In contrast, age, sex and smoking history were not associated with OS (P>0.05). Multivariate analysis further identified clinical stage, residual tumor and ERCC6L mRNA expression as independent risk factors of poor OS in patients with LUAD (P<0.001, P=0.001, and P=0.035, respectively). Moreover, univariate analysis showed that residual tumor (P=0.017) was associated with DFI, whereas age, sex, smoking history, and ERCC6L mRNA expression were not (P>0.05). Multivariate analysis showed that residual tumor (P=0.035) was an independent risk factor of poor DFI in patients with LUAD. In terms of DSS, univariate analysis showed that clinical stage, residual

Table II. Univariate and multivariate analysis of overall survival in 85 patients with LUAD.

Parameters	Univariate analysis				Multivariate analysis			
	HR	95% CI (lower/upper)		P-value	HR	95% CI (lower/upper)		P-value
Age (years) ≤65 vs. >65	1.186	0.688	2.045	0.539				
Sex Female vs. Male	0.888	0.532	1.480	0.648				
Tumor size T1/2 vs. T3/4	2.258	1.107	4.605	0.025[a]	1.506	0.708	3.205	0.288
Nodal invasion Yes vs. No	2.991	1.719	5.205	<0.001[a]	2.347	1.292	4.263	0.005[a]
Pathology grade I/II vs. III	1.144	0.669	1.959	0.623				
ERCC6L expression High vs. low	2.245	1.340	3.761	0.002[a]	1.771	1.041	3.013	0.035[a]

[a]P<0.05. LUAD, lung adenocarcinoma; HR, hazard ratio; CI, confidence interval; ERCC6L, excision repair cross-complementation group 6 like.

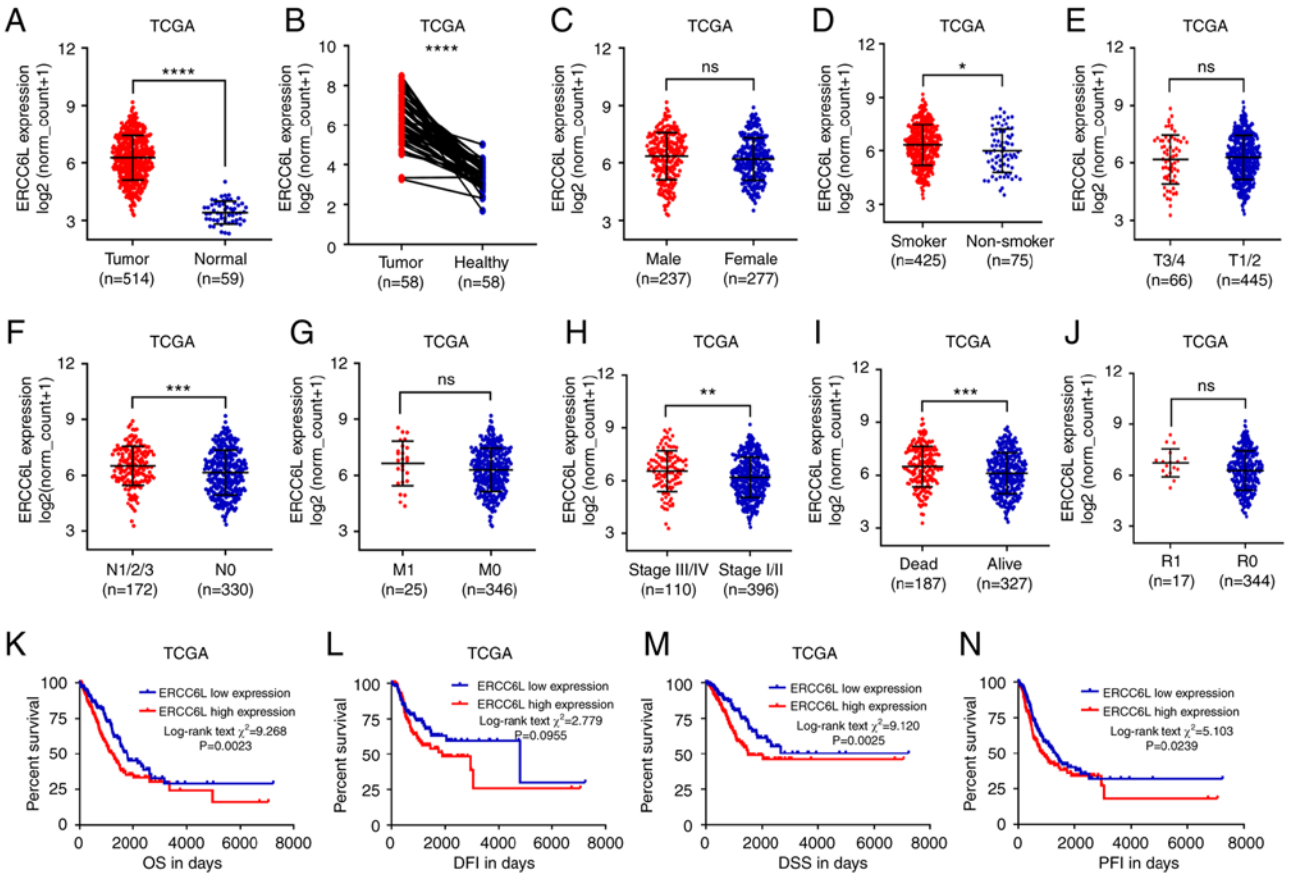

Figure 2. Association of ERCC6L mRNA expression with clinicopathological features and clinical outcomes in patients with LUAD based on the TCGA database. (A) Plot chart showing the mRNA expression levels of ERCC6L in LUAD tissues and normal lung tissues. (B) Plot chart showing the mRNA expression of ERCC6L in LUAD and paired normal tissues. (C-J) Plot chart showing ERCC6L mRNA expression between (C) male and female, (D) smoker and non-smoker, (E) cases with T3/4 and T1/2, (F) cases with or without nodal invasion, (G) cases with or without distant metastasis, (H) cases with stages III/IV and I/II, (I) live and dead cases, and (J) cases with or without residual tumor. (K-N) High ERCC6L RNA expression was associated with unfavorable outcomes in patients with LUAD. Kaplan-Meier curves of (A) OS, (B) DFI, (C) DSS and (D) PFI in cases with LUAD. *P<0.05, **P<0.01, ***P<0.001 and ****P<0.0001. ERCC6L, excision repair cross-complementation group 6 like; LUAD, lung adenocarcinoma; TCGA, The Cancer Genome Atlas; OS, overall survival; DFI, disease-free interval; DSS, disease-specific survival; PFI, progression-free interval; ns, not significant.

tumor and high ERCC6L mRNA expression were associated with DSS (P<0.001, P<0.001, and P=0.003, respectively). Multivariate analysis further identified clinical stage, residual tumor and ERCC6L mRNA expression as independent risk factors of poor DSS in patients with LUAD (P<0.001, P=0.001, and P=0.011, respectively). Univariate analysis revealed that clinical stage, residual tumor, and ERCC6L mRNA expression were associated with PFI (P=0.003, P<0.001, and P=0.029, respectively), whereas age, sex and smoking history were not (P>0.05). Multivariate analysis further confirmed that clinical

Table III. Univariate and multivariate analysis of OS, DFI, DSS and PFI in patients with LUAD in the TCGA database.

		Univariate analysis				Multivariate analysis			
	Parameters	HR	95% CI (lower/upper)		P-value	HR	95% CI (lower/upper)		P-value
OS	Age (Continuous)	1.008	0.992	1.023	0.330				
	Sex Female vs. Male	0.938	0.702	1.255	0.669				
	Smoking history 2/3/4/5 vs. 1	0.912	0.604	1.377	0.661				
	Clinical stage III/IV vs. I/II	2.651	1.945	3.613	<0.001[a]	2.400	1.748	3.295	<0.001[a]
	Residual tumors Yes vs. No	3.937	2.204	7.033	<0.001[a]	2.753	1.524	4.973	0.001[a]
	ERCC6L expression High vs. low	1.551	1.156	2.081	0.003[a]	1.771	1.041	3.013	0.035[a]
DFI	Age (Continuous)	1.016	0.994	1.039	0.158				
	Gender Female vs. Male	0.814	0.536	1.237	0.335				
	Smoking history 2/3/4/5 vs. 1	0.742	0.436	1.263	0.272				
	Clinical stage III/IV vs. I/II	0.803	0.371	1.740	0.578				
	Residual tumors Yes vs. No	4.108	1.281	13.170	0.017[a]	3.571	1.097	11.627	0.035[a]
	ERCC6L expression High vs. low	1.434	0.944	2.178	0.091	1.337	0.873	2.048	0.181
DSS	Age (Continuous)	0.998	0.970	1.007	0.206				
	Sex Female vs. Male	1.040	0.716	1.512	0.836				
	Smoking history 2/3/4/5 vs. 1	1.037	0.599	1.795	0.896				
	Clinical stage III/IV vs. I/II	2.472	1.662	3.676	<0.001[a]	2.131	1.420	3.199	<0.001[a]
	Residual tumors Yes vs. No	5.025	2.489	10.142	<0.001[a]	3.557	1.738	7.279	0.001[a]
	ERCC6L expression High vs. low	1.801	1.229	2.637	0.003[a]	1.670	1.125	2.480	0.011[a]
PFI	Age (Continuous)	0.998	0.984	1.012	0.733				
	Sex Female vs. Male	0.929	0.706	1.223	0.601				
	Smoking history 2/3/4/5 vs. 1	0.970	0.654	1.440	0.881				
	Clinical stage III/IV vs. I/II	1.622	1.180	2.230	0.003[a]	1.424	1.023	1.981	0.036[a]
	Residual tumors Yes vs. No	3.312	1.780	6.162	<0.001[a]	2.620	1.379	4.976	0.003[a]
	ERCC6L expression High vs. low	1.359	1.033	1.788	0.029[a]	1.330	1.004	1.762	0.047[a]

[a]P<0.05. Smoking history: 1, lifelong non-smoker; 2, current smoker; 3, current reformed smoker (for >15 years); 4, current reformed smoker (for ≤15 years); 5, current reformed smoker (duration not specified). OS, overall survival; PFI, progression-free interval; DFI, disease-free interval; DSS, disease-specific survival; LUAD, lung adenocarcinoma; TCGA, The Cancer Genome Atlas; HR, hazard ratio; CI, confidence interval; ERCC6L, excision repair cross-complementation group 6 like.

stage, residual tumor, and ERCC6L mRNA expression were independent risk factors of poor PFI in patients with LUAD (P=0.036, P=0.003, and P=0.047, respectively). The aforementioned results indicated that the upregulation of ERCC6L mRNA expression in TCGA-LUAD was negatively correlated with OS, DSS, and PFI.

Validation of the expression and clinical significance of ERCC6L in LUAD based on the GEO database. Data from the GEO database were used to validate the aforementioned results, and the independent array sets GSE30219 and GSE31210 were selected for analysis. In the GSE30219 dataset, there was no significant change in the mRNA expression levels of ERCC6L (P>0.05; Fig. 3A). However, in the GSE31210 microarray dataset, the mRNA expression levels of ERCC6L were significantly increased in LUAD tissue compared with normal lung tissue (P<0.001; Fig. 3B). LUAD tissues were divided into high- and low-expression groups according to the median mRNA expression of ERCC6L. Kaplan-Meier curve showed that, in the GSE30219 (Fig. 3C) and GSE31210 (Fig. 3D) datasets, the OS was significantly shorter in patients with high ERCC6L mRNA expression than in those with low ERCC6L mRNA expression. In addition, the area under the curve value of ERCC6L expression for the diagnosis of LUAD in the TCGA cohort was 0.9892 (P<0.0001). Meanwhile, in the GSE31210 array set, the area under the curve value of ERCC6L in LUAD was 0.9013 (P<0.0001; Fig. 3E).

Regulation of ERCC6L gene expression at DNA amplification and methylation levels. Deep sequencing data extracted from the TCGA database was used to investigate the potential mechanism involved in the dysregulation of the ERCC6L gene in LUAD. The association between ERCC6L mRNA expression and copy number data was examined in 69 LUAD cell lines from the Encyclopedia of Cancer Cell Lines. The results showed that the mRNA expression of ERCC6L was positively correlated with the DNA copy number (Fig. 3F). In addition, based on TCGA database, 71 patients (13.9%) had low or high DNA amplification, while 85 patients (16.6%) had DNA deletion (Fig. 3G). Furthermore, the correlation between ERCC6L

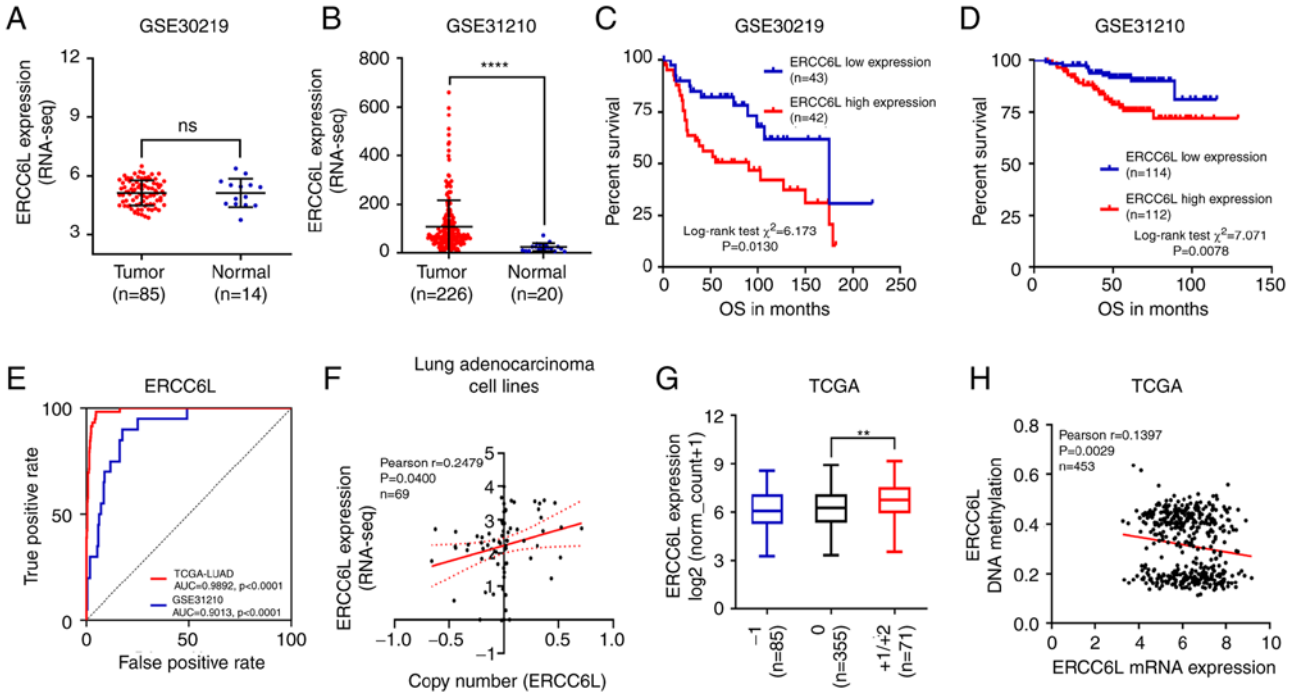

Figure 3. Validation of the role of ERCC6L in GEO datasets and exploration of genetic and epigenetic mechanisms of its dysregulation in LUAD. (A-E) ERCC6L mRNA expression profiles and prognostic significance in GEO dataset cohorts. The expression of ERCC6L mRNA in LUAD tissues and normal tissues from the (A) GSE30219 cohort and (B) GSE31210 cohort. Kaplan-Meier curves of OS in patients with LUAD using data from the (C) GSE30219 cohort and (D) GSE31210 cohort. (E) ROC curves showing the diagnostic value of ERCC6L mRNA expression in LUAD. (F) The expression of ERCC6L mRNA was correlated with copy number variation in LUAD cell lines based on the CCLE database (n=69; P=0.0400). (G) ERCC6L CNVs and mRNA expression in LUAD based on the TCGA database. DNA amplification was associated with ERCC6L mRNA expression. (H) Regression analysis of ERCC6L mRNA expression and DNA methylation level in LUAD based on the TCGA database (n=453; P=0.0029). **P<0.01 and ****P<0.0001. ERCC6L, excision repair cross-complementation group 6 like; GEO, Gene Expression Omnibus; LUAD, lung adenocarcinoma; OS, overall survival; ROC, receiver operating characteristic; CCLE, Cancer Cell Line Encyclopedia; CNVs, copy number variations; TCGA, The Cancer Genome Atlas.

mRNA expression and DNA methylation was examined in 453 patients with primary LUAD. The results showed that the mRNA expression of ERCC6L was negatively associated with DNA methylation in LUAD (Fig. 3H).

GSEA of genes co-expressed with ERCC6L in LUAD. To explore the potential functions and pathways of ERCC6L involvement in LUAD, RNA-seq data was analyzed from 515 patients with LUAD from TCGA database using LinkedOmics. The LinkFinder module of LinkedOmics was used to identify genes differentially expressed in correlation with ERCC6L in LUAD. The threshold was FDR <0.01 A volcano plot revealed differentially expressed genes positively (red dots) and negatively (green dots) correlated with ERCC6L in LUAD (Fig. 4A). The heat map showed the top 50 significant genes that were positively or negatively correlated with ERCC6L, respectively (Fig. 4B and C). As revealed in Fig. 4D, a very strong positive correlation was observed between ERCC6L expression and CDCA5 (r=0.8344), KIF4A (r=0.8743) and TPX2 (r=0.8464). Consistent with the ERCC6L gene, these three genes were upregulated in tumors and significantly associated with poor OS in patients with LUAD vs. normal controls (Fig. 4E and F).

Moreover, the LinkInterpreter module of LinkedOmics was used to conduct GSEA of genes co-expressed with ERCC6L in LUAD. The top 10 significant GO terms and signaling pathway enrichment results are presented in Fig. 5A and B. The results suggested that the genes positively co-expressed with ERCC6L were mainly located in the chromosomal regions of condensation, 'chromosomal region', 'spindle', and 'replication fork'. These genes are generally involved in 'chromosome segregation', 'DNA replication', 'chromatin assembly or disassembly', 'spindle organization' and 'cell cycle checkpoint'. Molecular function ontology analysis found that genes were mainly enriched in GO terms, such as 'catalytic activity acting on DNA', 'DNA helicase activity', 'single-stranded DNA binding' and 'DNA replication'. In addition, the KEGG pathway analysis showed that significant enrichment pathways were 'cell cycle', 'DNA replication', 'homologous recombination', 'oocyte meiosis', 'proteasome', 'spliceosome' and the 'P53 signaling pathway'.

Gene functional analysis of ERCC6L in LUAD at the single-cell level. Considering the heterogeneity among cancer cells, the biological functions of genes were further investigated at the single-cell level. The CancerSEA database was used to identify the main biological functions of ERCC6L in LUAD. As revealed in Fig. 5C, gene expression of ERCC6L was significantly correlated with the cell cycle, DNA repair, proliferation, DNA damage, invasion and EMT [P=0.49, 0.46, 0.43, 0.42, 0.33 (P<0.001) and 0.19 (P<0.05), respectively].

Construction of the ERCC6L gene-silencing LUAD cell line. The endogenous expression levels of ERCC6L mRNA and protein were examined in three LUAD cell lines, namely

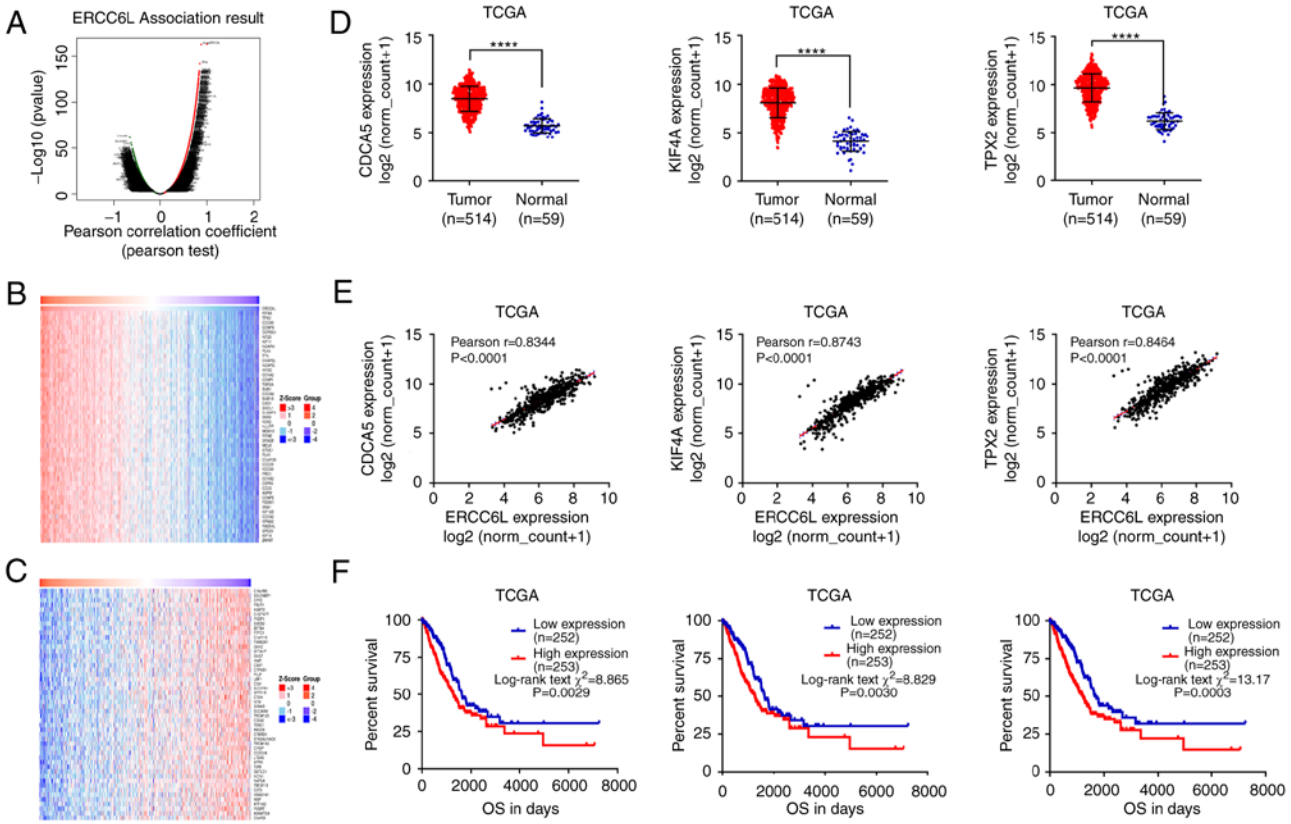

Figure 4. Differentially expressed genes are associated with ERCC6L in LUAD. (A) A volcano map showing significant correlation between differentially expressed genes and ERCC6L (FDR <0.01; P<0.05); (B and C) Heatmaps showing the top 50 significant genes (B) positively and (C) negatively correlated with ERCC6L in LUAD. (D-F) The top 3 significant genes positively co-expressed with ERCC6L in LUAD. (D) The mRNA expression levels of CDCA5, KIF4A, and TPX2 in LUAD tissues compared with normal lung tissues. (E) Pearson correlation of ERCC6L mRNA expression with CDCA5, KIF4A and TPX2. (F) Survival analyses of CDCA5, KIF4A and TPX2 in LUAD. ****P<0.0001. ERCC6L, excision repair cross-complementation group 6 like; LUAD, lung adenocarcinoma; TCGA, The Cancer Genome Atlas.

A549, H1975, and PC9. The results of qPCR and western blot analysis showed that ERCC6L was expressed in all three cell lines (Fig. 6A). Subsequently, the expression of endogenous ERCC6L in LUAD cell lines was knocked down using lentivirus-mediated shRNA. In this study, A549 and PC9 cells were selected for transfection with lentivirus, and stably transfected cells were constructed. The efficiency of interference with the ERCC6L gene was determined by qPCR and western blotting. The results showed that the efficiency of ERCC6L inhibition was 89 and 85% in A549 and PC9 cells, respectively (Fig. 6B). Knockdown of ERCC6L expression also inhibited ERCC6L protein expression in A549 and PC9 cells, respectively (Fig. 6C).

Effect of ERCC6L on the proliferation of LUAD cells. CCK-8 assay and plate clone formation assay were performed to assess the effect of ERCC6L on cell proliferation in LUAD. The results revealed that the downregulation of ERCC6L expression in A549 and PC9 cells decreased cell viability; the difference was statistically significant compared with the sh-NC group (Fig. 6D). In addition, knockdown of ERCC6L reduced the number and volume of A549 and PC9 cell clones and decreased the proliferation of these cells (Fig. 6E).

Effect of ERCC6L on cell apoptosis and the cell cycle of LUAD cells. Flow cytometric analysis was performed to explore the effects of ERCC6L on cell apoptosis and the cell cycle in LUAD. As revealed in Fig. 7A, the cell apoptotic rate of PC9 and A549 cells transfected with sh-ERCC6L was significantly higher than that of the control. In addition, following the downregulation of ERCC6L expression, the proportions of A549 and PC9 cells in the G1 phase decreased, while those in the S phase increased (Fig. 7B).

Effect of ERCC6L on cell migration and invasion of LUAD cells. Wound-healing and Transwell assays were performed to assess the effect of ERCC6L on cell migration and invasion in LUAD. The result of the wound-healing experiment showed that, compared with the sh-NC group, A549 and PC9 cells with ERCC6L knockdown showed significantly reduced migratory ability 24 and 48 h after the wound, as well as reduced wound-healing ability and relatively wide wound spacing (Fig. 8A). For the cell migration assay, the results revealed that the number of cells penetrating the membrane in the A549-sh-ERCC6L and PC9-sh-ERCC6L groups was significantly lower than that recorded in the NC group (P<0.0001 for both; Fig. 8B). Knockdown of ERCC6L could weaken the migratory ability of LUAD cells *in vitro*. For the cell invasion assay, compared with the sh-NC group, the number of A549 and PC9 cells transfected with sh-ERCC6L that penetrated the membrane was significantly decreased (P<0.001 for both; Fig. 8C). Collectively, these results suggested that knockdown

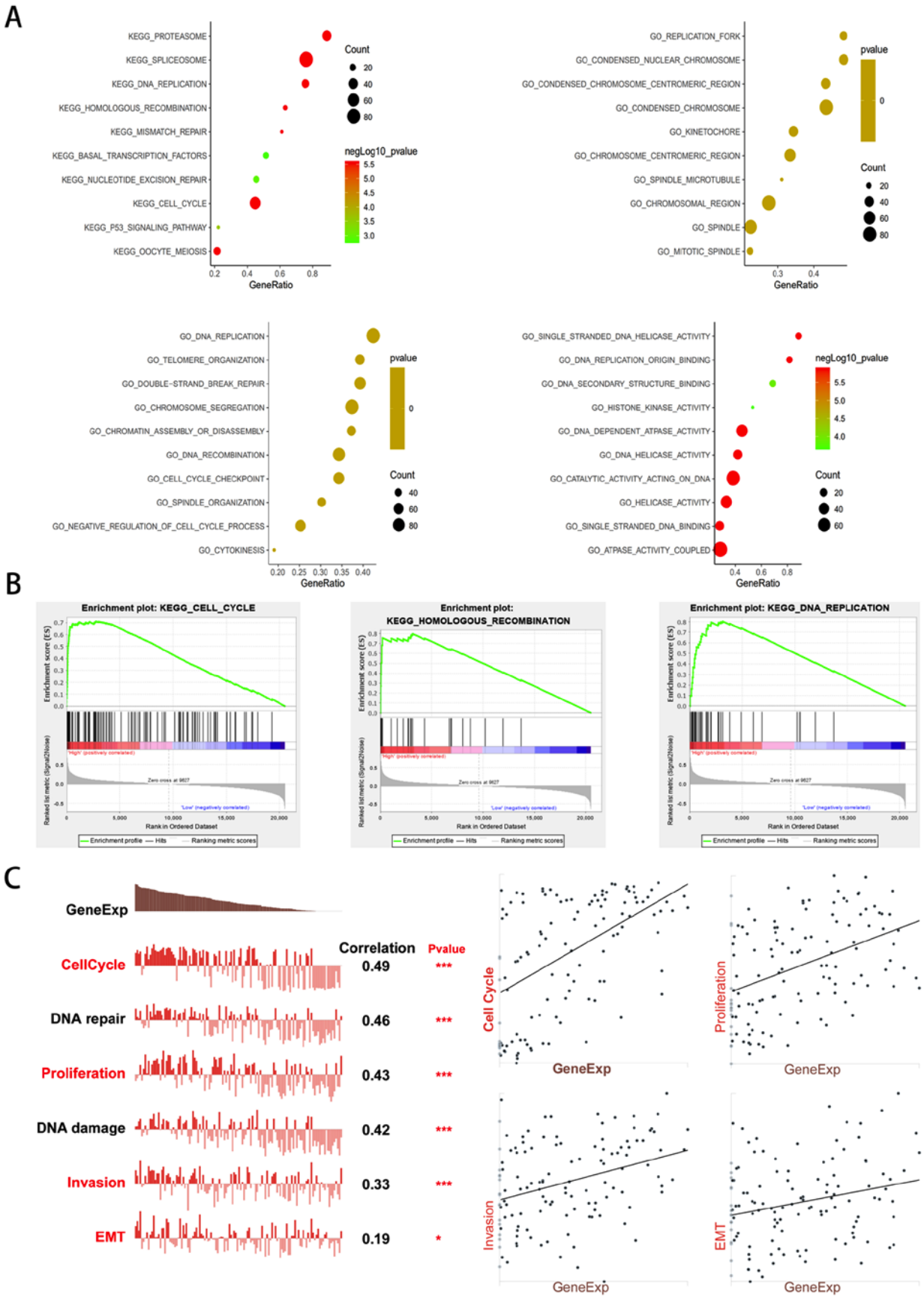

Figure 5. GSEA analysis and single-cell gene functional analysis of ERCC6L in LUAD. (A) Bubble plots showing the top 10 GO and KEGG pathway terms of genes co-expressed with ERCC6L in LUAD. (B) The top 3 KEGG pathways of genes positively co-expressed with ERCC6L in LUAD. ERCC6L upregulation was associated with 'cell cycle', 'homologous recombination' and 'DNA replication'. (C) Gene functional analysis of ERCC6L in LUAD at the single-cell level. Gene expression of ERCC6L was significantly correlated with cell cycle, DNA repair, proliferation, DNA damage, invasion, and EMT. Spearman's correlation was conducted. *P<0.05 and ***P<0.001. GSEA, gene set enrichment analysis; ERCC6L, excision repair cross-complementation group 6 like; LUAD, lung adenocarcinoma; GO, Gene Ontology; KEGG, Kyoto Encyclopedia of Genes and Genomes; EMT, epithelial-mesenchymal transition.

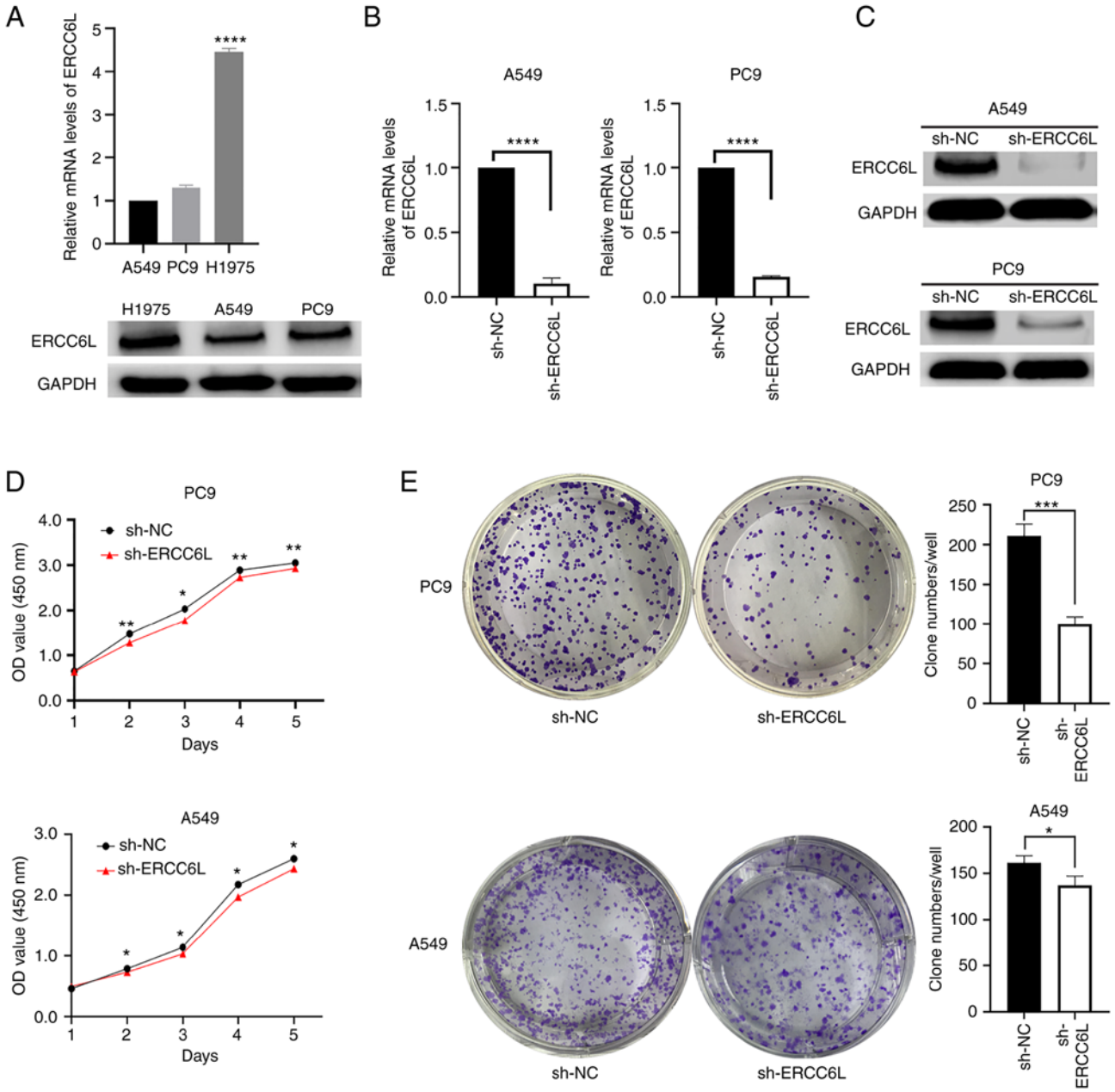

Figure 6. Knockdown of ERCC6L inhibits cell proliferation in LUAD *in vitro*. (A) The endogenous expression of ERCC6L mRNA and protein in A549, H1975 and PC9 cells was detected by qPCR and western blot analysis, respectively. (B) The transfection efficiency of lentivirus-mediated shRNA was verified by qPCR assay. Following knockdown of ERCC6L, the mRNA expression level was decreased in A549 and PC9 cells as detected by qPCR assay. (C) Following knockdown of ERCC6L, the protein expression level was downregulated in A549 and PC9 cells as detected by western blot analysis. (D) CCK-8 assay was performed to detect the proliferative activity of PC9 and A549 cells after silencing of ERCC6L. (E) Knockdown of ERCC6L inhibited the ability of plate clone formation in A549 and PC9 cells. *P<0.05, **P<0.01, ***P<0.001 and ****P<0.0001 compared with sh-NC. ERCC6L, excision repair cross-complementation group 6 like; LUAD, lung adenocarcinoma; qPCR, quantitative polymerase chain reaction; sh-, short hairpin; NC, negative control.

of ERCC6L could reduce the invasive ability of LUAD cells *in vitro*.

Association between ERCC6L and EMT, as well as the Wnt/β-catenin signaling pathway. To explore the potential molecular mechanism by which ERCC6L is involved in the progression of LUAD, the expression of EMT-related biomarkers and key molecules of the Wnt/β-catenin signaling pathway was examined. As revealed in Fig. 8D, compared with sh-NC, sh-ERCC6L decreased the protein expression levels of N-cadherin, Snai1 and Snai2 in A549 and PC9 cells, while it upregulated the protein expression levels of E-cadherin. Furthermore, knockdown of ERCC6L downregulated the expression levels of Notch 3 and β-catenin. These results suggested that ERCC6L may co-regulate EMT through the Wnt/β-catenin and Wnt/Notch 3 signaling pathways, thus affecting the occurrence and development of LUAD.

Effect of knocking down ERCC6L expression on the proliferation of LUAD cells in vivo. The aforementioned results showed that knockdown of ERCC6L inhibited the proliferation of LUAD cells *in vitro*. To verify if these results

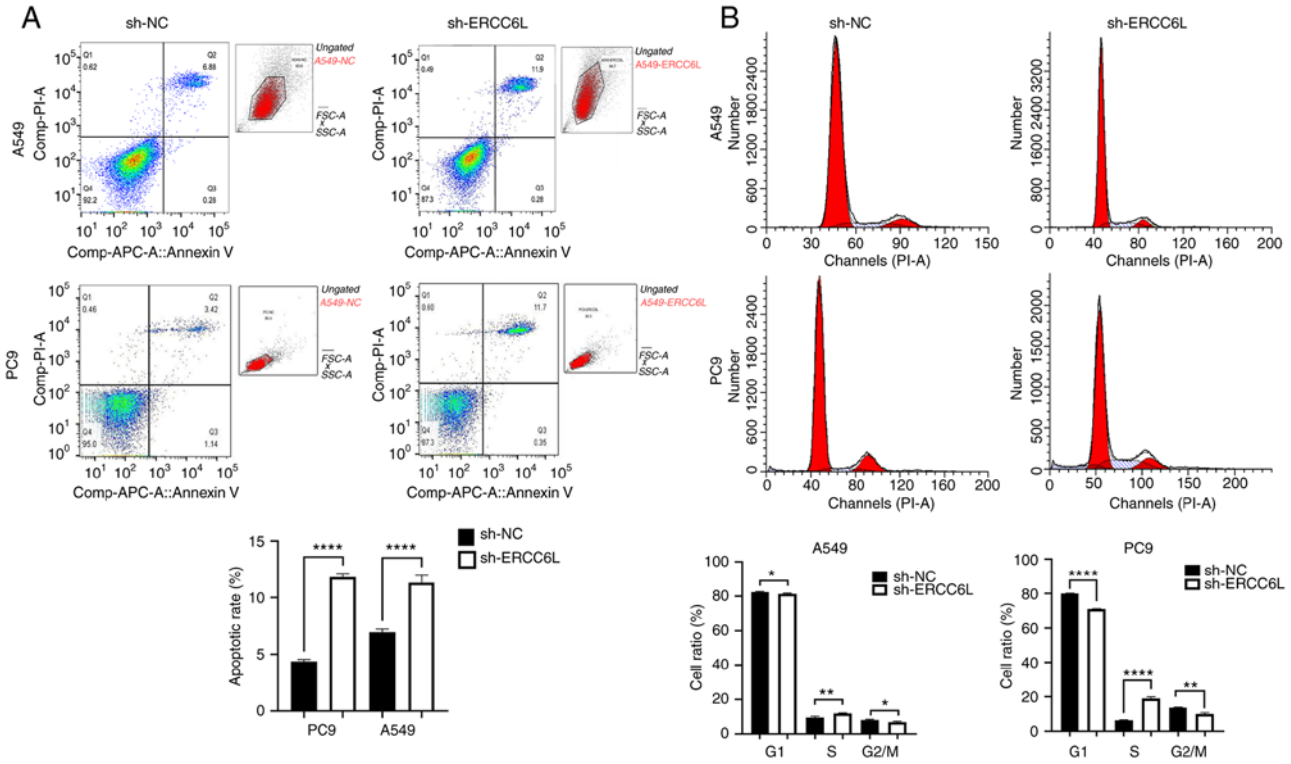

Figure 7. Knockdown of ERCC6L induces cell apoptosis and S-phase arrest in LUAD. (A) Annexin V/PI double-staining in the detection of apoptosis in A549 and PC9 cells by flow cytometry. Knockdown of ERCC6L increased the apoptosis rate of A549 and PC9 cells. (B) Effect of ERCC6L expression on the cell cycle distribution in LUAD. Following down-regulation of ERCC6L, the cell rate in the G1 and G2/M phase decreased, while the cell rate in the S phase increased. *P<0.05, **P<0.01 and ****P<0.0001. ERCC6L, excision repair cross-complementation group 6 like; LUAD, lung adenocarcinoma; sh-, short hairpin; NC, negative control.

are reproducible *in vivo*, a LUAD xenograft tumor model in nude mice was established. Tumorigenesis could be observed 4-7 days after inoculation. The state of the mice, including food intake, appeared to be normal throughout the experiment. As revealed in Fig. 8E, mice injected with sh-ERCC6L-transfected LUAD PC9 cells had reduced tumorigenicity, tumor volume and tumor weight compared with the control mice (P<0.05). In line with the *in vitro* findings, these results suggested that the low-expression of ERCC6L inhibited the proliferation of LUAD cells *in vivo*.

Discussion

The development of new genome-wide sequencing tests, as well as molecular targeted drugs and antibodies, has improved the overall efficacy of treatment against cancer. However, LUAD (a common type of lung cancer) is associated with poor prognosis and short survival. Therefore, it is necessary to investigate the mechanism involved in the tumorigenesis and progression of LUAD and further establish effective treatment strategies (30,31). In recent years, it has been consistently reported that the expression levels of SNF2 family members, ERCC6 and ERCC6L, are significantly associated with various types of cancers. For example, Zhao *et al* (32) reported that high expression of ERCC6 was associated with poor OS in patients with colorectal cancer who received or did not receive treatment with 5-fluorouracil. Luo *et al* (33) revealed that ERCC6 may be a biomarker for the prognosis of gastric cancer. Pu *et al* (34) demonstrated that the expression of ERCC6L was significantly correlated with the clinical survival of patients with breast and gastric cancer. Yu *et al* (35) revealed that liver cancer patients with low ERCC6L expression had significantly longer OS. Huang *et al* (36) also demonstrated the clinical potential of interfering with ERCC6L expression to improve the treatment of high-risk patients with triple-negative breast cancer. These studies suggested that ERCC6L is a valuable prognostic marker for patients with cancer and may be a prognostic biomarker. Nevertheless, little is known about the expression profile and function of ERCC6L in LUAD.

In this study, TCGA-RNA-seq data was initially used to demonstrate that ERCC6L is upregulated in most types of cancer, including LUAD. The immunohistochemical results based on paraffin sections revealed that ERCC6L was overexpressed in the tumor tissues of patients with LUAD. Subsequently, the clinical significance of ERCC6L expression in LUAD was further analyzed by integrating clinical samples with TCGA-LUAD data. The results showed that high ERCC6L expression was significantly associated with lymph node metastasis, TNM stage, and survival status. Therefore, ERCC6L may be involved in the carcinogenesis and progression of LUAD.

In clinical prognostic studies, objective OS events are typically considered the end point. This may affect clinical judgment due to the longer follow-up time for OS. For LUAD (a highly aggressive tumor type), using more accurate DFI, PFI, and DSS results with relatively short follow-up times as reference is of great importance. Because patients may relapse or deteriorate in a short period of time, this approach

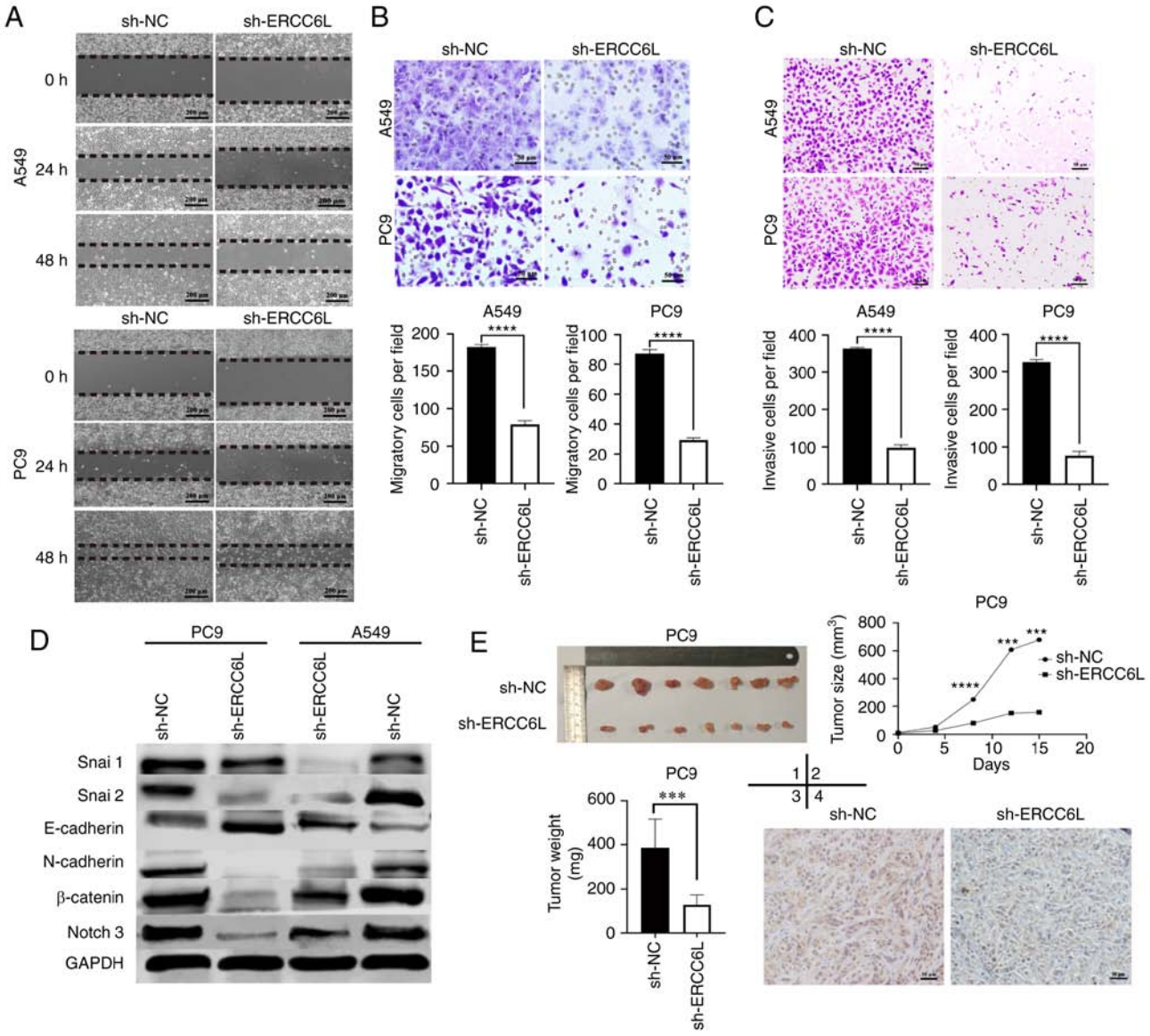

Figure 8. Effect of ERCC6L expression on cell migration, invasion, the EMT process and subcutaneous tumorigenesis of A549 and PC9 cells. (A) Representative images of A549 and PC9 cells transfected with sh-ERCC6L as detected by scratch assay. (B) Following knockdown of ERCC6L, Transwell migration assays were used to detect the migration ability of A549 and PC9 cells. (C) The BioCoat Matrigel invasion assay was used to examine the effect of ERCC6L on the invasion ability of A549 and PC9 cells. (D) Effect of ERCC6L expression on EMT marker molecules and nuclear transcription factors in LUAD cells. (E) Knockdown of ERCC6L inhibited growth of xenografted tumor in nude mice. (E-1) Representative image of subcutaneous xenografts of nude mice in sh-ERCC6L and sh-NC groups. (E-2,3) The tumor sizes and tumor weights of PC9 cells subcutaneous xenograft were compared between sh-ERCC6L and sh-NC groups. (E-4) Representative immunohistochemical staining of ERCC6L in subcutaneous tumors of nude mice (magnification, x400). ***P<0.001 and ****P<0.0001. ERCC6L, excision repair cross-complementation group 6 like; EMT, epithelial-mesenchymal transition; sh-, short haiprin; LUAD, lung adenocarcinoma; NC, negative control.

has practical guiding significance for biological research, such as tumor invasion and evaluation of clinical treatment effects. In the present study, high expression of ERCC6L in both LUAD clinical samples and the TCGA-LUAD dataset was significantly associated with shorter OS; this observation was consistent with the analysis of two GEO independent datasets. Cox regression analysis confirmed that ERCC6L expression was an independent risk factor affecting the prognosis of LUAD. Furthermore, in terms of PFI and DSS, ERCC6L was also indicated as an independent predicator in LUAD. In addition, the ROC analysis suggested that ERCC6L mRNA expression has certain diagnostic value. Collectively, these results suggest that ERCC6L is a promising biomarker for the diagnosis and prognosis of LUAD. This evidence also laid a foundation for further investigation on the function and mechanism of ERCC6L in LUAD.

Bioinformatics analysis can improve the reproducibility and effectiveness of diagnostic markers of cancer at different levels (e.g., molecular and pathway). In the present study, transcriptome data of LUAD was collected and epigenetic analysis, pathway analysis, and single-cell level analysis were performed to demonstrate that ERCC6L expression may affect the biological behavior of LUAD. To the best of our knowledge, the underlying molecular mechanisms of ERCC6L dysregulation in tumors are not yet fully understood. Considering the potential diagnostic and prognostic value of ERCC6L in

LUAD, it is important to explore the potential mechanism of ERCC6L dysregulation in LUAD. Genetic and epigenetic changes (e.g., CNVs, DNA methylation, and somatic mutations) often cause abnormalities in gene expression and cancer cell behavior. CNVs can regulate the expression of specific genes through a dose-effect relationship (37,38). In this study, DNA amplification was the main type that caused changes in ERCC6L and was positively correlated with upregulation of this gene. This association between CNVs and ERCC6L mRNA expression was also confirmed in LUAD cell lines. Therefore, it was hypothesized that the aberrant expression and dysregulation of ERCC6L in LUAD may be due to the alteration of chromosomal structure. In addition, ERCC6L mRNA expression was negatively correlated with methylation levels, indicating that ERCC6L expression may be modulated by DNA methylation in LUAD.

By identifying genes co-expressed with ERCC6L in LUAD, the possible biological roles and mechanisms of ERCC6L were further speculated from the perspective of gene enrichment analysis. The most significant positively correlated genes were CDCA5, KIF4A, and TPX2, which were overexpressed in tumor tissues of LUAD. These genes were positively correlated with ERCC6L expression and associated with poor OS. By GSEA analysis, these genes were revealed to be mainly concentrated in chromosomes, spindles, and microtubules and were primarily involved in cell cycle-related activities and regulation (e.g., mitotic cell cycle phase transition, chromosome separation, cell cycle checkpoint activity, etc.). Similarly, the cell cycle was the most significant signaling pathway for the enriched genes co-expressed with ERCC6L in LUAD. The cell cycle plays an important role in tumorigenesis (39). Dysregulation of the cell cycle can lead to cancer cell proliferation and tumor growth (40). Zhang *et al* (41) demonstrated that ERCC6L could enhance cell viability *in vitro* and promote tumor growth *in vivo* by regulating the mitogen-activated protein kinase (MAPK) signal transduction pathway after knockout of ERCC6L expression in 786-O cells. Chen *et al* (42) reported that ERCC6L promotes the development of liver cancer by activating the PI3K/AKT and nuclear factor-κB (NF-κB) signaling pathways. Nevertheless, whether ERCC6L affects the cell cycle of LUAD warrants further investigation.

Heterogeneity among cancer cells poses a major challenge to the diagnosis and treatment of cancer. Single-cell sequencing technology provides an unprecedented opportunity to accurately decipher the functional status of individual cancer cells (43). Functional analysis of ERCC6L in individual LUAD cells showed that overexpression of ERCC6L was positively correlated with the cell cycle, DNA repair, proliferation, DNA damage, invasion and EMT. The regulation of the cell cycle by ERCC6L overexpression was consistent with the results of the GSEA using data from the TCGA-LUAD dataset. In general, the results of the cancer cell line and single-cell analyses support the notion that the regulation of cell cycle progression may be the primary function of ERCC6L in LUAD cells.

Fernandez-Cuesta *et al* (43) showed that lung cancer types are not the result of early progenitor cell lesions of highly aggressive lung neuroendocrine tumors, instead, they arise through independent cellular mechanisms. Inactivation of chromatin remodeling genes is sufficient to drive lung carcinoid transformation. In fact, it has been shown that ERCC6L is involved in the remodeling of centromere chromatin, and its binding to PLK1 can enhance the function of ERCC6L in the consolidation of mitotic chromosomes (44-46). Notably, PLK1 plays an important role in cell division and proliferative life activities (36), indicating that the dysregulation of ERCC6L expression can lead to dysregulation of mitosis. In turn, this process affects the proliferative ability of cells. It has been reported that inactivation of ERCC6L gene results in p53 activation, DNA damage, and apoptosis in mouse embryos (47). It was hypothesized that ERCC6L plays an important role in the development of LUAD. Furthermore, continuous studies have shown that high expression of ERCC6L can promote abnormal cell proliferation and inhibit cell apoptosis in various malignant tumors, such as breast, gastric, and liver cancer. For example, knockdown of ERCC6L could significantly inhibit the proliferation of breast cancer cells and induce apoptosis *in vitro* (48). Pu *et al* (34) found that ERCC6L regulated the cell cycle through the RAB31/MAPK/cyclin dependent kinase 2 (CDK2) pathway and promoted the proliferation of cancer cells. Hence, it was hypothesized that ERCC6L may have a similar biological function in LUAD.

In the present study, a shRNA lentivirus was used to construct stable LUAD cell lines in which ERCC6L was knocked down. In cell function experiments, this method can achieve a relatively stable silencing effect of ERCC6L gene expression. Knockdown of ERCC6L inhibited the proliferation of A549 and PC9 cells *in vivo* and *in vitro*. Downregulation of ERCC6L expression lead to cell cycle arrest in the S phase and promoted apoptosis. These results indicated that the dysregulation of ERCC6L expression could affect the proliferative ability, apoptosis level, and cycle distribution of LUAD cells.

EMT is a process in which fully differentiated epithelial cells are transformed into mesenchymal phenotypes and plays an important role in embryonic development, wound healing and tumor invasion (49,50). EMT is a reversible process initiated by several factors, including TGF-β, Notch, Wnt, fibroblast growth factor (FGF), and epidermal growth factor (EGF) (51). In addition, the process is mediated by EMT-induced transcription factors, such as Snai1/2, Slug, Twist, zinc finger E-box binding homeobox 1 (ZEB1), and ZEB2. E-cadherin, N-cadherin, β-catenin, and Snai are important molecules involved in cell adhesion and EMT, and play important roles in organ formation, tissue homeostasis, and maintenance of epithelial integrity and polarity (52-54). Loss of E-cadherin function is associated with poor prognosis and survival in patients with various types of cancer (55). β-Catenin (a membrane adhesion protein complex) is an important component of the Wnt signaling pathway. Numerous studies have shown that mutations or dysregulation of components of the Wnt signaling pathway are associated with cancer in humans (56). The expression levels of E-cadherin and β-catenin play an important role in the occurrence of EMT in ovarian cancer cells (57,58). E-cadherin expression is downregulated in numerous cancer cell lines with enhanced invasion and migration phenotypes (59). The Wnt/β-catenin pathway directly or indirectly upregulates the expression of key transcription factors regulating E-cadherin (60). The Notch signaling pathway plays a key role in cell development, affecting cell processes (e.g., differentiation, proliferation and

migration) and participating in the occurrence and progression of cancer (61,62). Activation of EMT signaling in cancer cells is widely thought to contribute to metastasis, recurrence, or resistance to therapy; hence, molecules that regulate EMT are also considered drug targets (63). Changes in the occurrence and metastasis of lung cancer can be judged by changes in the levels of related EMT markers. Studies have shown that ERCC6L promotes the growth and invasion of colorectal cancer cells (64). Similarly, the present study demonstrated that inhibition of ERCC6L expression attenuated the migratory and invasive activities of A549 and PC9 cells. Following the downregulation of ERCC6L expression, the protein expression levels of N-cadherin, Snai1, Snai2, Notch 3, and β-catenin were decreased, whereas those of E-cadherin were increased. These results suggested that ERCC6L may influence the EMT of LUAD through the Wnt/β-catenin and Wnt/Notch 3 signaling pathways.

Clinically, LUAD is often diagnosed at an advanced stage; thus, it is difficult to determine the earliest time-point of EMT initiation. Currently, the effects of the expression of related genes on cell location remain unknown. Moreover, it is impossible to determine its influence on the treatment of tumors and their recurrence and metastasis after treatment. Therefore, discovering specific targets of epigenetic silencing during EMT is of great importance. The present study showed that ERCC6L is involved in regulating the changes in EMT, providing a new potential research target for the mechanism of EMT in LUAD.

In summary, ERCC6L was overexpressed in LUAD tissues compared with normal lung tissues. Increased expression of ERCC6L was significantly correlated with nodal invasion and advanced TNM staging, and acted as an independent risk factor for prognosis in patients with LUAD. DNA amplification and hypomethylation may contribute to ERCC6L dysregulation in LUAD. Knockdown of KIF18A inhibited LUAD cell proliferation *in vitro* and *in vivo*, attenuated cell migration and invasion, induced apoptosis and S-phase arrest. ERCC6L may regulate EMT through the Wnt/β-catenin and Wnt/Notch 3 signaling pathways, leading to malignant biological behavior (i.e., metastasis and invasion) of LUAD. Therefore, ERCC6L may be a potential therapeutic target for lung cancer. Nevertheless, there were several limitations in the present study. For example, only a few case samples were included in the studies on the association between the expression of ERCC6L and clinicopathological characteristics of patients; this is because fresh tissue samples need to be collected during surgery. Hence, the source of samples was limited, and the number of samples obtained was relatively small. Moreover, since the topic of the present study is that ERCC6L overexpression confers malignant phenotypes of LUAD, the effect of ERCC6L on normal cell lines (e.g., immortalized bronchial cells) should be further examined. Finally, the in-depth molecular mechanism involved in the genetic and epigenetic levels (e.g. DNA copy number and methylation), and in the promotion of lymph node metastasis and invasion of LUAD by ERCC6L remains to be fully elucidated.

Acknowledgements

The present study was jointly accomplished by The People's Hospital of Guangxi Zhuang Autonomous Region (also known as Guangxi Academy of Medical Sciences, Nanning, China) and Guangxi University. We are grateful to the Experimental Animal Center of Guangxi Medical University (Nanning, China) for the support of animal experiments. We would also like to thank the Research and Experiment Center of The People's Hospital of Guangxi Zhuang Autonomous Region for the support of cell and molecular biology experiments. We would also like to thank Dr Jiao Lan and Dr Mingzheng Mo from The People's Hospital of Guangxi Zhuang Autonomous Region for their excellent technical assistance.

Funding

The present study was supported by Guangxi Natural Science Foundation (grant no. 2018GXNSFBA281058), the Basic Ability Improvement Project of Young and Middle-aged Teachers in Guangxi Universities (grant no. 2018KY0050) and the National Natural Science Foundation of China (grant no. 82060078).

Availability of data and materials

The processed data required to reproduce these findings cannot be shared at this time as the data also form part of an ongoing study. Requests to access the datasets should be directed to the corresponding author YZ (yl.zhong@whu.edu.cn).

Authors' contributions

SL, LJ, XH, MY, HL, BL, ZW and YZ conceived and designed the study. XH, LJ, SL, ZW and YZ performed data curation. SL, HL, BL, MY and XH performed formal analysis of the data. XH, SL, LJ and YZ wrote the original draft of the manuscript. XH, SL, LJ, BL, HL, MY, and ZW wrote, reviewed and edited the final manuscript. SL, LJ and XH contributed equally to this work. SL, XH and YZ confirmed the authenticity of all the raw data. All authors contributed to the article and read and approved the submitted final version.

Ethics approval and consent to participate

The present study was approved (approval no. KY-KJT-2021-125) by the Ethics Committee of the People's Hospital of Guangxi Zhuang Autonomous Region (Nanning, China). All participants provided written informed consent in accordance with the Declaration of Helsinki. The animal experiment of this study was approved (approval no. 202103009) by The Animal Care and Welfare Committee of Guangxi Medical University (Nanning, China).

Patient consent for publication

Not applicable.

Competing interests

The authors declare that the research was conducted in the absence of any commercial or financial relationships that could be construed as potential competing interests.

References

1. Ferlay J, Colombet M, Soerjomataram I, Mathers C, Parkin DM, Piñeros M, Znaor A and Bray F: Estimating the global cancer incidence and mortality in 2018: GLOBOCAN sources and methods. Int J Cancer 144: 1941-1953, 2019.
2. Quintanal-Villalonga Á and Molina-Pinelo S: Epigenetics of lung cancer: A translational perspective. Cell Oncol (Dordr) 42: 739-756, 2019.
3. Kim D, Lee YS, Kim DH and Bae SC: Lung cancer staging and associated genetic and epigenetic events. Mol Cells 43: 1-9, 2020.
4. Santamaria A, Neef R, Eberspächer U, Eis K, Husemann M, Mumberg D, Prechtl S, Schulze V, Siemeister G, Wortmann L, *et al*: Use of the novel Plk1 inhibitor ZK-thiazolidinone to elucidate functions of Plk1 in early and late stages of mitosis. Mol Biol Cell 18: 4024-4036, 2007.
5. Xu Y, Chen X and Li Y: ERCC6L, a gene of SNF2 family, may play a role in the teratogenic action of alcohol. Toxicol Lett 157: 233-239, 2005.
6. Yin Y, Tang L, Zhang J, Tang B and Li Z: Molecular Cloning and Gene Expression Analysis of ERCC6L in Sika Deer (Cervus nippon hortulorum). PLoS One 6: e20929, 2011.
7. Baumann C, Körner R, Hofmann K and Nigg EA: PICH, a centromere-associated SNF2 family ATPase, is regulated by Plk1 and required for the spindle checkpoint. Cell 128: 101-114, 2007.
8. Bhola NE, Jansen VM, Bafna S, Giltnane JM, Balko JM, Estrada MV, Meszoely I, Mayer I, Abramson V, Ye F, *et al*: Correction: Kinome-wide functional screen identifies role of PLK1 in Hormone-independent, ER-positive breast cancer. Cancer Res 79: 876, 2019.
9. Helmke C, Becker S and Strebhardt K: The role of Plk3 in oncogenesis. Oncogene 35: 135-147, 2016.
10. Abbasi R, Ramroth H, Becher H, Dietz A, Schmezer P and Popanda O: Laryngeal cancer risk associated with smoking and alcohol consumption is modified by genetic polymorphisms in ERCC5, ERCC6 and RAD23B but not by polymorphisms in five other nucleotide excision repair genes. Int J Cancer 125: 1431-1439, 2009.
11. Hübner NC, Wang LH, Kaulich M, Descombes P, Poser I and Nigg EA: Re-examination of SiRNA specificity questions role of PICH and Tao1 in the spindle checkpoint and identifies Mad2 as A sensitive target for small RNAs. Chromosoma 119: 149-165, 2010.
12. Zhang G, Ma J, Xiong J, Huang X, Han X, Yu X and Jiang X: Upregulation of excision repair cross-complementation group 6-Like (ERCC6L) promotes tumor growth in hepatocellular carcinoma. Dig Dis Sci 66: 1097-1109, 2021.
13. Rami-Porta R, Asamura H, Travis WD and Rusch VW: Lung cancer-major changes in the American Joint Committee on Cancer eighth edition cancer staging manual. CA Cancer J Clin 67: 138-155, 2017.
14. Yamauchi M, Yamaguchi R, Nakata A, Kohno T, Nagasaki M, Shimamura T, Imoto S, Saito A, Ueno K, Hatanaka Y, *et al*: Epidermal growth factor receptor tyrosine kinase defines critical prognostic genes of stage I lung adenocarcinoma. PLoS One 7: e43923, 2012.
15. Rousseaux S, Debernardi A, Jacquiau B, Vitte AL, Vesin A, Nagy-Mignotte H, Moro-Sibilot D, Brichon PY, Lantuejoul S, Hainaut P, *et al*: Ectopic activation of germline and placental genes identifies aggressive metastasis-prone lung cancers. Sci Transl Med 5: 186ra66, 2013.
16. Mermel CH, Schumacher SE, Hill B, Meyerson ML, Beroukhim R and Getz G: GISTIC2. 0 facilitates sensitive and confident localization of the targets of focal somatic copy-number alteration in human cancers. Genome Biol 12: R41, 2011.
17. Nusinow DP, Szpyt J, Ghandi M, Rose CM, McDonald ER III, Kalocsay M, Jané-Valbuena J, Gelfand E, Schweppe DK, Jedrychowski M, *et al*: Quantitative proteomics of the cancer cell line encyclopedia. Cell 180: 387-402.e16, 2020.
18. Barretina J, Caponigro G, Stransky N, Venkatesan K, Margolin AA, Kim S, Wilson CJ, Lehár J, Kryukov GV, Sonkin D, *et al*: The cancer cell line encyclopedia enables predictive modelling of anticancer drug sensitivity. Nature 483: 603-607, 2012.
19. Chandrashekar DS, Bashel B, Balasubramanya SAH, Creighton CJ, Ponce-Rodriguez I, Chakravarthi BVSK and Varambally S: UALCAN: A portal for facilitating tumor subgroup gene expression and survival analyses. Neoplasia 19: 649-658, 2017.
20. Vasaikar SV, Straub P, Wang J and Zhang B: LinkedOmics: Analyzing multi-omics data within and across 32 cancer types. Nucleic Acids Res 46: D956-D963, 2018.
21. Tang Z, Kang B, Li C, Chen T and Zhang Z: GEPIA2: An enhanced web server for large-scale expression profiling and interactive analysis. Nucleic Acids Res 47: W556-W560, 2019.
22. Subramanian A, Tamayo P, Mootha VK, Mukherjee S, Ebert BL, Gillette MA, Paulovich A, Pomeroy SL, Golub TR, Lander ES and Mesirov JP: Gene set enrichment analysis: A knowledge-based approach for interpreting genome-wide expression profiles. Proc Natl Acad Sci USA 102: 15545-15550, 2005.
23. Kanehisa M and Goto S: KEGG: Kyoto encyclopedia of genes and genomes. Nucleic Acids Res 28: 27-30, 2000.
24. Ashburner M, Ball CA, Blake JA, Botstein D, Butler H, Cherry JM, Davis AP, Dolinski K, Dwight SS, Eppig JT, *et al*: Gene ontology: Tool for the unification of biology. The Gene Ontology Consortium. Nat Genet 25: 25-29, 2000.
25. Yuan H, Yan M, Zhang G, Liu W, Deng C, Liao G, Xu L, Luo T, Yan H, Long Z, *et al*: CancerSEA: A cancer single-cell state atlas. Nucleic Acids Res 47: D900-D908, 2019.
26. Livak KJ and Schmittgen TD: Analysis of relative gene expression data using real-time quantitative PCR and the 2(-Delta Delta C(T)) method. Methods 25: 402-408, 2001.
27. Gong HX, He L, Li XP, Wang YD, Li Y, Huang JJ, Wang Z, Xie D, Kung HF and Peng Y: Effective antitumor immunity against murine gliomas using dendritic cells transduced with hTERTC27 recombinant adenovirus. Oncol Rep 27: 1163-1169, 2012.
28. Yang Y, Guo Y, Tan S, Ke B, Tao J, Liu H, Jiang J, Chen J, Chen G and Wu B: β-Arrestin1 enhances hepatocellular carcinogenesis through inflammation-mediated Akt signalling. Nat Commun 6: 7369, 2015.
29. Lin CH, Wang CH, Hsu SL, Liao LY, Lin TA and Hsueh CM: Molecular mechanisms responsible for neuron-derived conditioned medium (NCM)-mediated protection of ischemic brain. PLoS One 11: e0146692, 2016.
30. Zhong Y, Jiang L, Lin H, Li X, Long X, Zhou Y, Li B and Li Z: Overexpression of KIF18A promotes cell proliferation, inhibits apoptosis, and independently predicts unfavorable prognosis in lung adenocarcinoma. IUBMB Life 71: 942-955, 2019.
31. Zhong Y, Jiang L, Long X, Zhou Y, Deng S, Lin H and Li X: Clinical significance and integrative analysis of kinesin family member 18B in lung adenocarcinoma. OncoTargets Ther 12: 9249-9264, 2019.
32. Zhao Z, Zhang G and Li W: Elevated Expression of ERCC6 confers resistance to 5-fluorouracil and is associated with poor patient survival in colorectal cancer. DNA Cell Biol 36: 781-786, 2017.
33. Luo SS, Liao XW, Zhu XD and Doetsch PW: Prognostic value of excision repair cross-complementing mRNA expression in gastric cancer. Biomed Res Int 2018: 6204684, 2018.
34. Pu SY, Yu Q, Wu H, Jiang JJ, Chen XQ, He YH and Kong QP: ERCC6L, A DNA helicase, is involved in cell proliferation and associated with survival and progress in breast and kidney cancers. Oncotarget 8: 42116-42124, 2017.
35. Yu B, Liang H, Ye Q and Wang Y: Upregulation of ERCC6L is associated with tumor progression and unfavorable prognosis in hepatocellular carcinoma. J Gastrointest Oncol 11: 1009-1023, 2020.
36. Huang Y, Li W, Yan W, Wu J, Chen L, Yao X, Gu F, Lv L, Zhao J, Zhao M, *et al*: Loss of PICH promotes chromosome instability and cell death in triple-negative breast cancer. Cell Death Dis 10: 428, 2019.
37. Gamazon ER and Stranger BE: The impact of human copy number variation on gene expression. Brief Funct Genomics 14: 352-357, 2015.
38. Gao Y and Teschendorff AE: Epigenetic and genetic deregulation in cancer target distinct signaling pathway domains. Nucleic Acids Res 45: 583-596, 2017.
39. Ingham M and Schwartz GK: Cell-cycle therapeutics come of age. J Clin Oncol 35: 2949-2959, 2017.
40. Malumbres M and Barbacid M: Cell cycle, CDKs and cancer: A changing paradigm. Nat Rev Cancer 9: 153-166, 2009.
41. Zhang G, Yu Z, Fu S, Lv C, Dong Q, Fu C, Kong C and Zeng Y: ERCC6L That Is Up-regulated in high grade of renal cell carcinoma enhances cell viability in vitro and promotes tumor growth in vivo potentially through modulating MAPK signalling pathway. Cancer Gene Ther 26: 323-333, 2019.

42. Chen H, Wang H, Yu X, Zhou S, Zhang Y, Wang Z, Huang S and Wang Z: ERCC6L Promotes the progression of hepatocellular carcinoma through activating PI3K/AKT and NF-κB signaling pathway. BMC Cancer 20: 853, 2020.
43. Fernandez-Cuesta L, Peifer M, Lu X, Sun R, Ozretić L, Seidal D, Zander T, Leenders F, George J, Müller C, *et al*: Frequent mutations in chromatin-remodelling genes in pulmonary carcinoids. Nature Commun 5: 3518, 2014.
44. Kurasawa Y and Yu-Lee LY: PICH and cotargeted Plk1 coordinately maintain prometaphase chromosome arm architecture. Mol Biol Cell 21: 1188-1199, 2010.
45. Rouzeau S, Cordelières FP, Buhagiar-Labarchède G, Hurbain I, Onclercq-Delic R, Gemble S, Magnaghi-Jaulin L, Jaulin C and Amor-Guéret M: Bloom's Syndrome and PICH Helicases cooperate with topoisomerase IIα in centromere disjunction before anaphase. PLoS One 7: e33905, 2012.
46. Leng M, Besusso D, Jung SY, Wang Y and Qin J: Targeting Plk1 to chromosome arms and regulating chromosome compaction by the PICH ATPase. Cell Cycle 7: 1480-1489, 2008.
47. Albers E, Sbroggiò M, Pladevall-Morera D, Bizard AH, Avram A, Gonzalez P, Martin-Gonzalez J, Hickson ID and Lopez-Contreras AJ: Loss of PICH results in chromosomal instability, p53 activation, and embryonic lethality. Cell Rep 24: 3274-3284, 2018.
48. Liu J, Sun J, Zhang Q and Zeng Z: shRNA knockdown of DNA Helicase ERCC6L expression inhibits human breast cancer growth. Mol Med Rep 18: 3490-3496, 2018.
49. Greenburg G and Hay ED: Epithelia suspended in collagen gels can lose polarity and express characteristics of migrating mesenchymal cells. J Cell Biol 95: 333-339, 1982.
50. Nawshad A, LaGamba D, Polad A and Hay ED: Transforming growth factor-beta signaling during epithelial-mesenchymal transformation: Implications for embryogenesis and tumor metastasis. Cells Tissues Organs 179: 11-23, 2005.
51. Otsuki Y, Saya H and Arima Y: Prospects for new lung cancer treatments that target EMT signaling. Dev Dyn 247: 462-472, 2018.
52. Vu T and Datta PK: Regulation of EMT in colorectal cancer: A culprit in metastasis. Cancers (Basel) 9: 171, 2017.
53. Kaszak I, Witkowska-Piłaszewicz O, Niewiadomska Z, Dworecka-Kaszak B, Ngosa Toka F and Jurka P: Role of cadherins in cancer-a review. Int J Mol Sci 21: 7624, 2020.
54. Shook D and Keller R: Mechanisms, mechanics and function of epithelial-mesenchymal transitions in early development. Mech Dev 120: 1351-1383, 2003.
55. Wong SHM, Fang CM, Chuah LH, Leong CO and Ngai SC: E-cadherin: Its dysregulation in carcinogenesis and clinical implications. Crit Rev Oncol Hematol 121: 11-22, 2018.
56. Tafrihi M and Nakhaei Sistani R: E-Cadherin/β-catenin complex: A target for anticancer and antimetastasis plants/plant-derived compounds. Nutr Cancer 69: 702-722, 2017.
57. Al-Alem L and Curry TE Jr: Ovarian cancer: Involvement of the matrix metalloproteinases. Reproduction 150: R55-R64, 2015.
58. Kenny HA and Lengyel E: MMP-2 functions as an early response protein in ovarian cancer metastasis. Cell Cycle 8: 683-688, 2009.
59. Mendonsa AM, Na TY and Gumbiner BM: E-cadherin in contact inhibition and cancer. Oncogene 37: 4769-4780, 2018.
60. Nguyen VHL, Hough R, Bernaudo S and Peng C: Wnt/β-catenin signalling in ovarian cancer: Insights into its hyperactivation and function in tumorigenesis. J Ovarian Res 12: 122, 2019.
61. Artavanis-Tsakonas S, Rand MD and Lake RJ: Notch signaling: Cell fate control and signal integration in development. Science 284: 770-776, 1999.
62. Siebel C and Lendahl U: Notch signaling in development, tissue homeostasis, and disease. Physiol Rev 97: 1235-1294, 2017.
63. O'Leary K, Shia A and Schmid P: Epigenetic regulation of EMT in non-small cell lung cancer. Curr Cancer Drug Targets 18: 89-96, 2018.
64. Xie Y, Yu J, Wang F, Li M, Qiu X, Liu Y and Qi J: ERCC6L Promotes Cell Growth and Invasion in Human Colorectal Cancer. Oncol Lett 18: 237-246, 2019.